The γδ T cell receptor combines innate with adaptive immunity by utilizing spatially distinct regions for agonist-selection and antigen responsiveness

Daisy Melandri[1,2,8], Iva Zlatareva[1,2,8], Raphaël A.G. Chaleil[3], Robin J. Dart[1,2,7], Andrew Chancellor[4], Oliver Nussbaumer[5], Oxana Polyakova[5], Natalie A. Roberts[1,2], Daniela Wesch[6], Dieter Kabelitz[6], Peter M. Irving[7], Susan John[1], Salah Mansour[4], Paul A. Bates[3], Pierre Vantourout[1,2,*], and Adrian C. Hayday[1,2,*].

[1]Peter Gorer Department of Immunobiology, School of Immunology & Microbial Sciences, King's College London, SE19RT, UK. [2]Immunosurveillance Laboratory, The Francis Crick Institute, London, NW11AT, UK. [3]Biomolecular Modelling Laboratory, The Francis Crick Institute, London, NW11AT, UK. [4]Academic Unit of Clinical and Experimental Sciences, Faculty of Medicine, University of Southampton, SO166YD, UK. [5]GammaDelta Therapeutics, London BioScience Innovation Center, NW10NH, UK. [6]Institute of Immunology, University Hospital Schleswig-Holstein, Christian-Albrechts University, Kiel, 24105, Germany. [7]Department of Gastroenterology, Guy's and St Thomas' Foundation Trust, London, SE19RT, UK.

[8]These authors contributed equally to this study.

[*]Co-corresponding authors: pierre.vantourout@kcl.ac.uk; adrian.hayday@kcl.ac.uk

ABSTRACT

T cell receptor (TCR) γδ-expressing T lymphocytes compose evolutionarily conserved cells with paradoxical features. On the one hand, clonally expanded γδ T cells with unique specificities typify adaptive immunity. Conversely, large TCRγδ^{+} intraepithelial lymphocyte (γδ IEL) compartments exhibit limited TCR diversity and effect rapid, innate-like tissue surveillance. The development of several γδ IEL compartments depends upon epithelial *Btnl*/*BTNL* (butyrophilin-like) genes, which are members of the *B7*-superfamily of T cell co-stimulators. Here we show that Btnl/BTNL responsiveness is mediated by germline-encoded motifs within the cognate TCRVγ chains of mouse and human γδ IEL. This contrasts with diverse antigen recognition by clonally-restricted complementarity-determining regions (CDRs) 1-3 of TCRγδ. Hence, TCRγδ intrinsically combines innate and adaptive immunity by utilizing spatially distinct regions to discriminate non-clonal agonist-selecting elements from clone-specific ligands. The broader implications for antigen receptor biology are considered.

INTRODUCTION

Adaptive immunity in jawed vertebrates is underpinned by the use of somatic gene rearrangement to diversify three conserved lineages of lymphocytes: αβ T cells, B cells and γδ T cells[1]. *Prima facie*, TCRγδ has high intrinsic diversity, and major expansions of unique γδ T cell clones have been described, with cytomegalovirus (CMV) a candidate driver[2, 3, 4].

Nonetheless, microbe-specific γδ T cells have proved largely elusive. Instead, human peripheral blood γδ T cells make generic responses to microbes by recognizing hydroxymethylbut-2-enyl pyrophosphate (HMBPP), an intermediate in sterol metabolism that is more akin to a pathogen-associated molecular pattern[5]. Indeed, HMBPP-reactive cells also respond to endogenous sterol intermediates, e.g. isopentenyl pyrophosphate (IPP), upregulated in virus-infected or transformed cells[5,5]. Likewise, the TCR specificities of rare or unique mouse and human γδ T cells are seemingly enriched in self-encoded ligands, several of which are closely related to Major Histocompatibility Complex (MHC) proteins[6, 7, 8, 9, 10, 11]. Until the biological significance of such specificities is established, the host benefits of adaptive γδ TCR diversification will remain unresolved.

In contrast to clonally-restricted reactivities, the Vγ5Vδ1 TCR of murine dendritic epidermal T cells (DETC) is quasi-monoclonal. Likewise, most murine intestinal IEL express Vγ7[12, 13, 14]. Such extra-lymphoid γδ T cells exhibit hallmarks of innate immunity, in providing rapid, non-clonal responses to local tissue dysregulation[15, 16, 17, 18]. The acquisition of innate-like properties by T cells has been associated with agonist selection during development[19], in which regard, $V\gamma5^+$ DETC development

depends on *Skint1,* a *Btnl* gene expressed by thymic epithelial cells and suprabasal keratinocytes[20, 21]. Likewise, Vγ7$^+$ IEL development depends on *Btnl1* expressed by enterocytes[22]. Moreover, consistent with Btnl/BTNL proteins functioning as heteromers[23], Vγ7$^+$ IEL respond specifically to cells co-expressing Btnl1 and Btnl6. Indicative of a conserved biology, human colonic γδ T cells specifically respond to cells co-expressing the enterocyte proteins, BTNL3 and BTNL8[22].

Btnl/BTNL proteins sit within the B7-superfamily, whose members link innate and adaptive immunity by communicating the prevailing pathophysiologic milieu (e.g. the presence of microbes) to lymphocyte co-receptors, such as CD28[16]. As an example, Skint1 structurally resembles PD-L1, a B7-related ligand for the PD1 inhibitory co-receptor[24]. Hence, Btnl/BTNL proteins might likewise regulate γδ T cells *via* co-receptors. Conversely, the strict associations of Btnl/BTNL proteins with γδ TCR usage might reflect their acting directly *via* the TCR. Indeed, TCR Vγ9Vδ2-mediated HMBPP/IPP responses are BTN3A1+BTN3A2-dependent[23, 25]. The prospect that some γδ TCRs might be specific for monomorphic, self-encoded proteins while others show clonally-restricted reactivities has provoked the view that there are both innate and adaptive γδ T cells[26].

Here we offer a different perspective, in showing that signature, murine and human intestinal γδ TCRs are sufficient to confer responsiveness to discrete, Btnl/BTNL proteins. However, the response is mediated by a germline-encoded segment of Vγ that neither contributes to nor obviously precludes antigen-binding to clonally-restricted CDRs. Thus, individual γδ TCRs have an intrinsic capacity to combine innate and adaptive immunity consistent with the multifaceted biology of γδ T cells.

RESULTS

Murine TCRVγ7 mediates Btnl-responsiveness

The signature intestinal γδ IEL compartment is dominated by $V\gamma7^+$ cells, whose development is severely impaired in *Btnl1*$^{-/-}$ mice[22]. To assess the diversity of *Btnl1*-dependent $V\gamma7^+$ cells, a small-scale TCR deep-sequencing analysis[22] was expanded, revealing that $V\gamma7^{CDR3}$ varied in length (from 10-15 amino acids) and slightly in sequence composition (Fig. 1a). TCRδ chain usage was diverse, mostly comprising four gene segments, particularly when only unique reads were counted so as to correct for clonal expansions: *Trdv2-2* (encoding the Vδ4 chain recognized by monoclonal antibody GL2[27]); *Trdv7*; *Trdv6D-1* and *Trdv6D-2* (Fig. 1b). In each case, CDR3δ length and composition were highly diverse (Fig. 1c). Of note, $V\gamma7^-$ IELs, which are a minor fraction of gut γδ T cells and are *Btnl1*-independent, showed largely comparable Vδ chain usage, albeit that *Trdv1* and *Trdv5* were relatively enriched (Supplementary Fig. 1a). In sum, deep sequencing revealed Vγ7 gene segment usage to be the sole constant property of *Btnl1*-dependent IEL.

When MODE-K murine intestinal epithelial cells were transduced with *Btnl1* and *Btnl6*, the gene products showed stoichiometric co-immunoprecipitation (Supplementary Fig. 1b), in relation to which primary $V\gamma7^+$ IEL specifically down-regulate their TCRs when co-cultured with MODE-K *Btnl1*+*Btnl6*-transductants (MODE-K.l1l6 hereafter), but not with MODE-K cells transduced with either *Btnl1* or *Btnl6* alone or with empty vector (MODE-K.EV)[22]. To explore the basis of this, co-cultures were optimized such that ≥50% of $V\gamma7^+$ IEL upregulated CD25 (IL-2Rα chain), of which most cells downregulated CD122 (the interleukin 15 (IL-15) receptor

β chain), downregulated the TCR by ~40%, and upregulated CD71 (the transferrin receptor) relative to cells co-cultured with MODE-K.EV (Fig. 1d-f). Such phenotypic changes are typical for T cells experiencing TCR engagement[28].

Based on the clear discrimination between Btnl1+6-responsive and non-responsive $V\gamma7^{+}$ IEL offered by this assay, we performed single cell flow cytometry-sorting of responding cells, and (informed by the deep sequencing data) subjected them to gene amplification with TCRVγ7, Vδ7, Vδ2-2 and Vδ6D1/2 primers, followed by sequencing. Consistent with the deep sequencing data, the forty-three TCRγ/δ pairs obtained showed $V\gamma7^{CDR3}$ lengths of 12-15 amino acids, paired to unique clones of Vδ7 (n=25), Vδ2-2 (n=13) and Vδ6D1/2 (n=5) with diverse CDR3δ lengths and sequences (Supplementary Table 1). $V\gamma7^{+}$ IEL diversity was evident in the uniqueness of each γ/δ pairing, although some limits were suggested by our finding that ~25% of recovered TCRδ sequences were also identified in the deep sequencing data-sets derived from three independent IEL harvests (Supplementary Table 1).

Capturing this TCR diversity, we stably transduced J76 cells, a human TCR-deficient T cell line that can be used to assay TCR bio-activities[29], with seven Vγ7Vδ pairs, mo1-mo7, that collectively spanned three different Vδ chains, with six being represented in the deep sequencing data-sets (Table 1). Each pairing was efficiently and comparably expressed on the cell surface, as was a control Vγ5Vδ1 DETC TCR, termed moD (Fig. 2a). When incubated with anti-CD3ε, a TCR cross-linking agent, J76-mo1 through J76-mo7 cells showed substantial TCR downregulation relative to transductants cultured with isotype-control antibody (Fig. 2b, c). The expression of

CD25 and CD122 by J76 cells were not reliably modulated by anti-CD3ε, precluding their use as read-outs of TCR responsiveness. However, all transductants upregulated CD69 in response to anti-CD3ε, albeit variably (Fig. 2b, c). Of note, TCR downregulation occurs rapidly in response to TCR engagement, whereas CD69 upregulation is a downstream event, which segregated qualitatively but not quantitatively with TCR downregulation (Fig. 2c).

J76-mo1 through J76-mo7 cells phenocopied primary Vγ7$^+$ IEL by showing TCR downregulation of ~35% to ≥50% upon co-culture with MODE-K.l1l6 cells but not MODE-K.EV cells (Fig. 2b, c). In all cases, CD69 was upregulated, again correlating qualitatively rather than quantitatively with TCR downregulation (Fig.2b, c). Conversely, Vγ5Vδ1$^+$ J76-moD cells showed neither TCR downregulation nor CD69 upregulation when co-cultured with MODE-K.l1l6 cells (Fig. 2b, c). However, responsiveness to MODE-K.l1l6 cells was qualitatively restored for J76-mo5.Vδ1 cells expressing a variant of moD in which the Vγ5 chain was replaced with the mo5 Vγ7 chain (the most common Vγ7 sequence in the three deep-sequencing analyses) (Table 1) (Fig. 2c). The fact that J76-mo5.Vδ1 cells responded less well than J76-mo5 cells (Fig 2c) most likely reflected the fact that the Vδ1 chain (encoded by the *Trdv4* gene) never ordinarily pairs with Vγ7: indeed, there was no *Trdv4* read in the deep-sequencing data of sorted Vγ7$^+$ cells (Fig. 1b). From these results, we conclude that different IEL-derived Vγ7$^+$ TCRs are sufficient to make human J76 cells qualitatively responsive to mouse Btnl1+6, largely irrespective of Vδ usage and CDR3γ/δ composition. Nonetheless, different, comparably expressed Vγ7$^+$ TCRs

showed quantitative variation in responsiveness both to Btnl1+6 and to anti-CD3ε (Fig. 2c).

The comparable kinetics of CD69 upregulation by J76-mo5 cells stimulated with either MODE-K.l1l6 cells or anti-CD3ε (Supplementary Fig. 2a) further suggested that the Vγ7-dependent responses reflected TCR engagement. Likewise, *NR4A1*, a signature TCR-responsive gene encoding the transcription factor Nur77[30] was substantially and significantly upregulated by J76-mo5 cells exposed to anti-CD3ε or MODE-K.l1l6 cells, but not to MODE-K.EV cells (Fig. 2d), phenocopying the response of primary IEL from *Nur77.eGFP* transgenic mice[22].

To preclude that responsiveness to MODE-K.l1l6 cells reflected some unexplained facet of TCR-transduced J76 cells, we transduced mo1 and mo5 TCRs (Table 1) into TCR-deficient human JRT3 cells expressing an NFAT activation-dependent luciferase[31]. Following co-culture with MODE-K.l1l6 cells, but not MODE-K.EV cells, JRT3-mo1 and JRT3-mo5 cells showed TCR downregulation, CD69 upregulation, and induced luciferase activity: conversely, no such responses were shown by Vγ5Vδ1$^+$ JRT3-moD cells (Supplementary Fig. 2b). Similarly, exposure to anti-CD3ε or to MODE-K.l1l6 cells provoked IL-2 secretion as well as moderate TCR downregulation and CD69 upregulation by the Jurkat subclone E6.1 transduced with mo5 (Supplementary Fig. 2c). In sum, the capacity of the mouse Vγ7$^+$ mo5 TCR to confer Btnl1+6 responsiveness to several human T cell lines strongly suggested that reactivity was mediated by the TCR itself. Moreover, J76-mo5 cells, J76-mo1 cells, and primary Vγ7$^+$ IEL responded to Btnl1+6 expressed by live or fixed cells, and by cells of different origins (human gut [MODE-K] and kidney [293T];

hamster ovary [CHO]; mouse skin [PAM2.12]) (Supplementary Fig. 2d-g), making it unlikely that the Vγ7$^+$ TCR-mediated response was to undefined molecule(s) co-expressed with Btnl1+6.

TCR-mediated BTNL-responsiveness is conserved

Like their Vγ7$^+$ mouse counterparts, human colonic γδ T cells located primarily to the IEL compartment (Fig. 3a) and responded *ex vivo* to 293T cells specifically co-transduced with human *BTNL3*+*BTNL8*, primarily expressed by gut epithelial cells[22]. To investigate the basis of this responsiveness, we optimized the co-culture of primary colonic T cells with BTNL3+8-expressing 293T cells (293T.L3L8 hereafter). Across several healthy donors, the predominant gut γδ T cell population, reactive to an antibody specific for Vγ2, Vγ3 and Vγ4 chains[32] (Supplementary Fig. 3a), showed consistent TCR downregulation of ~45%, and variable CD25 upregulation relative to cells incubated with 293T.EV cells (Fig. 3b; Supplementary Fig. 3b). These responses were not observed in colonic Vγ2/3/4$^-$ γδ T cells, Vδ2$^+$ T cells (typical of blood γδ cells) or αβ T cells (Fig. 3b; Supplementary Fig. 3b).

This optimized assay permitted BTNL3+8 responsive γδ T cells to be single cell-sorted based on TCR downregulation (Donor 1) or TCR downregulation and CD25 upregulation (Donors 2 and 3) (Fig. 3c). The nineteen TCRγδ pairs (hu1-hu19) recovered from the BTNL3+8 responsive cells were dominated by Vγ4 chains (17/19) with variable CDR3 composition and length (from 9-14 amino acids), paired to either Vδ1 (12/19) or Vδ3 (7/19) chains displaying highly diverse CDR3s (Table 2). Although all 19 recovered sequences were unique, ~50% were identified in the deep sequencing data sets, albeit at different frequencies (Table 2).

Three Vγ4Vδ1^{+} TCR pairs - hu7, hu12, and hu17 - displaying diverse CDR3γ/δ sequences and ranging from high abundance to very rare in the deep-sequencing reads (Table 2), were cloned and used to transduce J76 cells (hereafter J76-hu7, J76-hu12, J76-hu17), while a peripheral blood-derived Vγ9Vδ2 TCR was used to generate a control cell line, J76-huPB. Displaying reasonably comparable levels of surface expression (Supplementary Fig. 3c), J76-hu7, J76-hu12, and J76-hu17 cells showed pronounced TCR downregulation in response to anti-CD3ε or co-culture with 293T.L3L8 cells, but not 293T.EV cells (Fig. 3d, e). CD69 was likewise upregulated, although the magnitude varied across the three transductants in response to 293T.L3L8 cells or anti-CD3ε (Fig. 3d,e). Conversely, J76-huPB cells showed neither TCR downregulation nor CD69 upregulation (Fig. 3e). Of note, TCR downregulation by J76-hu transductants responding to 293T.L3L8 cells was usually greater than that shown by J76-mo transductants responding to MODE-K.l1l6 cells (compare Fig 2c and Fig 3e), possibly reflecting the differential signaling modalities of human and mouse γδTCRs[33].

J76-hu12 cells responded to BTNL3+8 expressed by different cell types, including human J76 T cells and murine MODE-K cells (Supplementary Fig. 3d). Likewise, JRT3 cells (see above) transduced with hu12 showed NFAT activation-dependent luciferase activity following exposure to either 293T.L3L8 cells or PMA+ionomycin, whereas control Vγ9Vδ2^{+} JRT3.huPB cells responded only to PMA+ionomycin (Supplementary Fig. 3e). These data indicated that the constant feature of BTNL3+8 responsive cells was Vγ4.

BTNL-responsiveness requires TCR FR3/HV4

Two of the 19 TCRγδ pairs recovered from the single-cell sorted, BTNL-responsive human colonic γδ T cells expressed Vγ2, which differs from Vγ4 by only nine amino acids (Fig. 4a). It was therefore important to test whether Vγ2 could also confer BTNL3+8 responsiveness, or whether the recovery of $V\gamma2^{+}$ TCRs was from cells stochastically expressing low TCR levels during the sort. To this end, J76 cells were transduced with a modified version of hu17 (hu17.Vγ2) in which the Vγ4 gene segment was substituted with the Vγ2 chain, while preserving CDR3γ and the same Vδ1 chain (Supplementary Fig. 4a). The resultant transductants showed neither TCR downregulation nor CD69 upregulation in response to co-culture with 293T.L3L8 cells (Fig. 4b and Supplementary Fig. 4b).

Three of the amino acid differences between Vγ2 and Vγ4 map to CDR1 and CDR2 (Fig. 4a). Therefore, J76 cells were transduced with modified versions of hu17 in which Vγ4 CDR1 and/or CDR2 were replaced with the counterpart Vγ2 sequences (hu17.$V\gamma2^{CDR1}$; hu17.$V\gamma2^{CDR2}$; and hu17.$V\gamma2^{CDR1+2}$) (Supplementary Fig 4a). Upon co-culture with 293T.L3L8 cells, the resulting transductants showed TCR downregulation and CD69 upregulation comparable to J76-hu17 cells (Fig. 4b and Supplementary Fig. 4b), indicating that the failure of Vγ2 to respond to BTNL3+8 did not map to the CDRs.

Vγ2 also differs from Vγ4 by four amino acids in a sub-region of framework region 3 (FR3) known as "hypervariable region 4" (HV4) because of its variability among different antigen receptors (Fig 4a). When J76 cells were transduced with a modified version of hu17 in which $V\gamma2^{HV4}$ (KY**Y**TY**A**STR**N**NLR**L**IL, hereafter referred to as

YANL) (Supplementary Fig. 4a) replaced the Vγ4 counterpart (KY**D**TY**G**STR**K**NLR**M**IL, hereafter DGKM), the resulting transductants (hu17$^{DGKM>YANL}$ cells) showed neither TCR downregulation nor CD69 upregulation in response to 293T.L3L8 cells (Fig. 4c and Supplementary Fig. 4c), pinpointing the importance of HV4.

Of the four amino acids distinguishing Vγ4^{HV4} from Vγ2^{HV4} (DGKM *versus* YANL), exchanging only the two most N-terminal residues (hu17.$^{DG>YA}$) was sufficient to abrogate BTNL3+8 responsiveness, whereas exchanging the remaining two residues (hu17.$^{KM>NL}$) (Supplementary Fig. 4a) was well tolerated (Fig. 4c and Supplementary Fig. 4c). Reciprocally, inserting DG from Vγ4^{HV4} in place of YA in Vγ2^{HV4} (hu17.Vγ2$^{YA>DG}$) (Supplementary Fig. 4a) was sufficient to confer strong BTNL3+8-responsiveness on J76-hu17.Vγ2$^{YA>DG}$ cells (Fig. 4d and Supplementary Fig. 4d). The Vγ3 gene segment is further diverged from Vγ4 than is Vγ2 (Fig. 4a). Thus, J76-hu17.Vγ3 cells transduced with a variant of hu17 in which Vγ3 was substituted for Vγ4 predictably failed to show TCR downregulation or CD69 upregulation CD69 when co-cultured with 293T.L3L8 cells (Fig. 4d and Supplementary Fig. 4a, d). However, J76-hu17.Vγ3-Vγ4^{HV4} cells, in which Vγ3^{HV4} was replaced by Vγ4^{HV4} partially recovered responsiveness (Fig. 4d and Supplementary Fig. 4a, d). Completely consistent results were obtained in parallel when NFAT-dependent luciferase activity was measured in JRT3 cells transduced with hu17, hu17$^{DG>YA}$, hu17.Vγ2, hu17.Vγ2$^{YA>DG}$, hu17.Vγ3, and hu17.Vγ3-Vγ4^{HV4} (Supplementary Fig. 4e). Collectively these results show that the N-terminal portion of Vγ4^{HV4} was necessary and sufficient for transduced T cells to respond to 293T.L3L8 cells, although its potency was evidently modified by other sequences within the Vγ gene segment.

The role of FR3/HV4 is evolutionarily conserved

Next we investigated the basis of the Btnl1+6 responsiveness of mouse Vγ7 TCRs. Although mouse Vγ genes differ greatly from each other, Vγ6 shares some similarities with Vγ7, in particular the properties of the amino acids surrounding the CDRs and the length of the serine-rich CDR2 (Fig. 5a). Therefore, J76 cells were transduced with mo5.Vγ6, in which Vγ7 was replaced with Vγ6, while still retaining the $V\gamma7^{CDR3}$ (Fig 5a). J76-mo5.Vγ6 cells expressed the Vγ6Vδ2-2 TCR at the cell surface, albeit at slightly lower levels than J76-mo5 cells (Supplementary Fig. 5a, b), but they neither downregulated the TCR nor upregulated CD69 in response to MODE-K.l1l6 cells (Fig. 5b and Supplementary Fig. 5b). In contrast, cells transduced with mo5.$V\gamma6^{CDR1}$ in which the $V\gamma7^{CDR1}$ (RTGTY) was replaced with $V\gamma6^{CDR1}$ (TSVQKPDAY) (Fig 5a) showed only partially reduced Btnl1+6 responsiveness relative to J76-mo5 cells (Fig. 5b and Supplementary Fig. 5a, b). Btnl1+6 responsiveness was also retained, albeit reduced, when mo5 $V\gamma7^{CDR2}$ (YNFVSSTT) was substituted with $V\gamma6^{CDR2}$ (SSSKENI) (mo5.$V\gamma6^{CDR2}$), or when both CDR1 and CDR2 of Vγ7 were replaced by the equivalent regions from Vγ6 (mo5.$V\gamma6^{CDR1+2}$) (Fig.5a,b and Supplementary Fig. 5a, b). In sum, CDR1 and CDR2 residues were not essential for Btnl1+6 responsiveness.

Because mouse Vγ7 is more closely related to human Vγ4 and Vγ2 than to any other mouse Vγ gene, sequence alignment allowed us to identify four residues, (H,E,K,F) in mouse $V\gamma7^{HV4}$ (KY**H**VY**E**GPD**K**RYK**F**VL) that corresponded to the four residues (D,G,K,M) at which human $V\gamma4^{HV4}$ differed from $V\gamma2^{HV4}$ (Supplementary Fig. 5c), two of which (D and G) were shown to be essential for BTNL3+8 responsiveness (see Fig 4c). Based on this, J76 cells were transduced with a construct (mo5$^{HEF>DGM}$) in

which the mouse Vγ7 residues, HEKF, were replaced with their human Vγ4 counterparts, DGKM (Supplementary Fig. 5c). When co-cultured with MODE-K.l1l6 cells, these J76-mo5$^{HEF>DGM}$ cells showed neither TCR downregulation nor CD69 upregulation (Fig 5c and Supplementary Fig. 5d). Likewise, mo5 constructs carrying single amino acid exchanges between Vγ7^{HV4} and human Vγ4^{HV4} (mo5$^{H>D}$ and mo5$^{E>G}$) (Supplementary Fig. 5c) identified two residues (H and E) in the N-terminal portion of Vγ7^{HV4} that were essential for responding to Btnl1+6 (Fig. 5c and Supplementary Fig. 5d), and that occupied equivalent positions to the two determinants (D and G) of human Vγ4 responsiveness to BTNL3+8. Indeed, whereas replacement of Vγ7^{HV4} in mo5 with human Vγ4^{HV4} (mo5-huVγ4^{HV4}) (Supplementary Fig 5c) abrogated Btnl1+6 responsiveness, there was a compensatory gain of responsiveness (TCR downregulation and CD69 upregulation) toward cells expressing human BTNL3+8 (Fig. 5d). Thus, BTNL/Btnl responsiveness is determined by FR3/HV4 motifs whose positioning is evolutionarily conserved, and which are functionally interchangeable.

BTNL3 and Btnl6 CFG faces interact with HV4

The molecular structure of the human Vγ4Vδ1 TCR (PDB 4MNG)[7] revealed that HV4 formed a solvent-exposed loop (Supplementary Fig. 6a). Because we occasionally observed TCR downregulation and CD69 upregulation in co-cultures of Vγ4Vδ1 transductants with 293T.L3 cells but never with 293T.L8 cells (Fig. 6a), we investigated whether the Vγ4 HV4 loop might mediate responses to solvent-exposed residues of BTNL3 *versus* BTNL8. To this end, a model for the BTNL3+8 dimer was derived from the X-ray structure of a BTN3A1 homodimer (PDB 4F80)[34] using an in-house homology program, 3D-JIGSAW[35] (Supplementary Fig. 6b). Second, for each

modeled chain, sequence alignments allowed beta-strand demarcation (A, B, C, C', C", D, E, F) according to the convention for Ig superfamily members (Supplementary Fig. 6c, d). Third, candidate solvent-exposed motifs that differed between the N-terminal IgV-domains of BTNL3 and BTNL8 were identified as: NQFHA/GQFSS; EDWESK/KDQPFM; WF/RI; and DEEAT/YQKAI in the C, C", F, and G strands, respectively (Fig. 6b, Supplementary Fig. 6c). Fourth, unrestricted docking simulations between Vγ4 and the BTNL3 IgV-domain using the in-house, publicly available docking server SwarmDock[36] produced solutions converging on an interaction of $V\gamma4^{HV4}$ with the CFG face of BTNL3 (Supplementary Fig. 6e) that harbors three of the sets of residues distinguishing BTNL3 from BTNL8. Of note, Ig-fold CFG faces are established mediators of protein-protein interactions[37].

Based on these findings, HA-tagged BTNL8 was co-expressed in 293T cells with either FLAG-tagged BTNL3 or with each of four FLAG-tagged BTNL3 constructs in which the candidate C, C'', F, and G motifs were replaced with counterpart BTNL8 sequences ($L3^{GQFSS}$, $L3^{KDQPFM}$, $L3^{RI}$, $L3^{YQKAI}$) (Fig 6c). Although each was comparably expressed (Supplementary Fig. 6f), only 293T.L3L8 cells and 293T.$L3^{KDQPFM}$L8 cells would induce TCR downregulation and CD69 upregulation in co-cultured J76-hu17 cells (Fig 6c). These results, together with the solutions offered by SwarmDock (above), permitted us to propose a refined docked complex in which unique residues in the CFG face of BTNL3 mediated functional interactions with $V\gamma4^{HV4}$ (Fig. 6d).

Recombinant, monomeric, human Vγ4Vδ2 or Vγ4Vδ1 soluble TCRs (sTCRs), but neither Vγ2Vδ1 nor Vγ8Vδ1 sTCRs, showed dose-dependent staining of 293.L3L8

cells but not of 293T.EV cells (Fig. 6e,f), indicating that TCR Vγ4 can interact specifically and directly with BTNL3+8. Consistent with this, the Vγ4Vδ2 and Vγ4Vδ1 sTCRs specifically stained mouse MODE-K.L3L8 cells (Supplementary Fig. 6g). Of note, the lower mean fluorescence intensity of MODE-K.L3L8 staining relative to 293T.L3L8 cell staining correlated with the relative expression of BTNL3+8 on the two cell types (Supplementary Fig. 6h).

Next, we identified motifs on the CFG faces of mouse Btnl1 and Btnl6 corresponding to the BTNL3 residues that interact with $V\gamma4^{HV4}$ (Supplementary Fig. 6i,j). Thereupon, we generated 293T cells co-expressing Btnl1 with either Btnl6 or each of three mutants in which the Btnl6 C, F, G strand residues were replaced by their Btnl1 counterparts ($l6^{AQPTP}$, $l6^{Q}$, $l6^{SQEVS}$) (Fig 6g). Likewise we generated 293T cells co-expressing Btnl6 with either Btnl1 or mutants in which the Btnl1 C, F, G strand residues were replaced by Btnl6 counterparts ($l1^{SRFSA}$, $l1^{H}$, $l1^{YEEAI}$) (Fig 6g). Only 293T cells expressing wild type Btnl6 provoked TCR downregulation and CD69 upregulation by co-cultured J76-mo5 cells, whereas 293T cells expressing mutant forms of Btnl6 did not (Fig. 6g and Supplementary Fig. 6k). In sum, these results revealed that functional interactions with mouse $TCRV\gamma7^{HV4}$ and human $TCRV\gamma4^{HV4}$, respectively, were mediated by amino acid motifs in evolutionarily conserved positions on the C, F, G faces of Btnl6 and BTNL3, respectively. In both cases, the motifs mapped to only one of the two Btnl/BTNL chains required for activity.

Human and mouse γδTCRs show dual reactivity

The human Vγ4Vδ1 TCR structure used for modeling was previously shown to react to a CD1d-sulfatide complex, largely *via* $V\delta1^{CDR1-3}$. According to our refined docked

complex model (Fig. 6d), the Vγ4Vδ1 TCR could simultaneously engage CD1d-sulfatide and BTNL3+8 expressed by the same cell (Fig. 7a). To further investigate this prospect of dual TCR-reactivity, we used a Vγ4Vδ5 TCR derived from LES, a human γδ T cell clone that responds to CMV-infected cells and to a spectrum of human carcinomas, including gut-derived HT29 cells[8]. These TCR-dependent responses are attributable to a unique specificity for a CD1-related protein, EPCR (endothelial protein C receptor), mediated largely by $V\gamma4^{CDR3}$.

We found that JRT3 cells transduced with the LES TCR (JRT3-LES), but not JRT3-hu12 cells showed significant, albeit low TCR downregulation and substantial CD69 upregulation when co-cultured with either HT29 cells or 293T cells over-expressing EPCR (293T.EPCR) (Fig. 7b). CD69 upregulation was completely or partially inhibited when the co-cultures were supplemented with an anti-EPCR antibody (Supplementary Fig. 7a). By contrast, JRT3-LES and JRT3-hu12 cells both showed TCR downregulation and CD69 upregulation when co-cultured with 293T.L3L8 cells or 293T.EPCR+L3L8 cells, that each over-express BTNL3+8. Moreover, this response was unaffected by EPCR-reactive antibodies (Fig. 7b and Supplementary Fig. 7a). Thus, JRT3-LES cells displayed a clonally-restricted TCR reactivity towards EPCR and a non-clonal TCR reactivity towards BTNL3+8.

Relative to co-cultures with 293T.EV cells, JRT3-LES cells co-cultured with 293T.EPCR, 293T.L3L8, or 293T.EPCR+L3L8 cells showed activation within 5 minutes of PLC-γ and p-LAT, as judged by Western blotting (Supplementary Fig. 7b), thereby indicating that activation *via* either of the LES TCR specificities (EPCR and BTNL3+8) could converge on equivalent downstream signaling pathways.

Because the Vγ4Vδ5 LES TCR is blood-derived, the results also indicated that BTNL3+8 reactivity extended beyond gut-derived Vγ4 TCRs. Indeed, J76 cells transduced with two human skin-derived Vγ4Vδ1 TCRs (sk1 and sk2) also showed TCR downregulation and CD69 upregulation when co-cultured with 293T.L3L8 cells (Supplementary Fig. 7c). Thus, seemingly irrespective of their tissue-of-origin, TCRVγ4 chains drove non-clonal responses to BTNL3+8.

To examine if dual reactivity could be observed in primary intestinal γδ T cells from a healthy donor, colonic Vδ1$^+$ IEL were sorted on the basis of binding to dextrameric multimers of CD1c complexed to phosphatidylcholine (CD1c-PC) (Supplementary Fig 7d). Of 24 Vδ1$^+$ cells sorted and subjected to TCR sequencing, twenty one were Vγ5Vδ1$^+$ and two were Vγ8Vδ1$^+$, but one was Vγ4Vδ1$^+$, from which the TCR (hu20) (Table 2) was used to transduce J76 cells. J76-hu20 cells, but not J76-hu17 cells could be stained specifically by CD1c-PC (Fig. 7c), whereas both cells lines showed strong responsiveness to 293T.L3L8 cells (Fig. 7d). Thus, J76-hu20 cells showed clonally-restricted TCR binding of CD1c-PC and non-clonal BTNL3+8 responsiveness.

Lastly, we examined if dual reactivity also extended to primary mouse intestinal γδ IEL, ~0.5% of which reportedly bind to the MHC class I-related molecule T10-T22 *via* a specific CDR3δ motif [6]. The same CDR3δ motif was found in the Vγ7Vδ7 TCR of mo8 (clone 24, Supplementary Table 1), and J76-mo8 cells showed TCR downregulation and CD69 upregulation in response to cells over-expressing T22 (MODE-K.T22; 293T.T22) as well as to cells over-expressing Btnl1+6 (MODE-K.l1l6; 293T.l1l6; MODE-K.T22+l1l6; and 293T.T22+l1l6) (Fig. 7e and Supplementary Fig. 7e). Moreover, Western blotting showed specific activation of

PLCγ and pLAT in J76-mo8 cells co-cultured with MODE-K.l1l6, MODE-K.T22, and MODE-K.T22+l1l6 cells (Supplementary Fig. 7f). Conversely, J76-mo5 cells responded only to Btnl1+6-expressing cells (Fig. 7e). Thus, J76-mo8 cells showed clonally-restricted responsiveness to T22 and non-clonal TCR responsiveness to Btnl1+6. Recognition by J76-mo8 cells of 293T.T22 cells (Fig. 7f) showed that the clonally-restricted response did not depend on Btnl1+6 proteins, since they were not expressed by 293T cells.

DISCUSSION

Here we identify an evolutionarily conserved mechanism by which the γδ TCR mediates the regulation of mouse and human intestinal γδ IELs by Btnl/BTNL proteins. Murine $V\gamma7^{+}$ and human $V\gamma4^{+}$ TCRs were sufficient to confer qualitative responsiveness to Btnl1+6 and to BTNL3+8, respectively, whereas TCRs expressing different Vγ gene segments did not. Complementary loss-of-function and gain-of-function experiments mapped Btnl/BTNL responsiveness to equivalent positions in the germline-encoded HV4 regions of mouse Vγ7 and human Vγ4, respectively. Thus, specific TCRVγ regions can use germline motifs to mediate responses to endogenous agonists, suggesting an innate interaction germane to the heritability of TCRVγ genes.

Molecular modeling identified a means by which human $V\gamma4^{HV4}$ might interact directly with the CFG face of the N-terminal IgV domain of BTNL3. Supporting that model were mutagenesis studies that likewise implicated the CFG face of the Btnl6 IgV domain in engaging mouse $V\gamma7^{HV4}$. Of note, CFG faces mediate heterotypic interactions of numerous Ig superfamily proteins, including CD2, CD4, VCAM and

MADCAM[38, 39, 40, 41]. These results suggest a conserved mechanism whereby BTNL/Btnl regulation of γδ IEL is mediated by an "interacting chain" (Btnl6 or BTNL3) coupled to a "supporting chain" (Btnl1 or BTNL8) that jointly determine biological activity. Moreover, this conservation may extend to the collaborative regulation by BTN3A1 and BTN3A2 of human peripheral blood γδ T cell responses to HMBPP[23].

Beyond the requirement for mouse Vγ7 and human Vγ4, respectively, Btnl/BTNL-responsive γδ IEL are diverse, expressing various TCRδ chains with diverse CDR3s. According to the structural modeling, those clone-specific CDR3 regions could remain available to engage clonally-restricted antigens, irrespective of Btnl/BTNL engaging HV4. Consistent with this, we demonstrated dual specificities for two human BTNL-responsive Vγ4 TCRs and for a murine Btnl-responsive Vγ7 TCR, with different sub-regions of the CDRs implicated in ligand binding [9,24]. Such spatially discrete dual specificities, involving HV4 and CDRs1-3, respectively, are distinct from commonly described cross-reactivities of CDR1-3 regions in other types of antigen receptor. Rather, the γδ TCR has an intrinsic capacity to use a discrete germline-encoded region to mediate innate, non-clonal responses to an endogenous agonist, and recombinase-dependent regions to mediate adaptive, clone-specific responses to diverse ligands. Clearly, these findings offer a framework for reconciling the innate-like biologies of γδ T cells with their adaptive, highly individual clonal dominance patterns[2, 3, 4].

BTNL/Btnl RNAs are seemingly expressed by differentiated enterocytes. Thus, following γδ IEL selection Btnl/BTNL proteins might sustain steady-state interactions

with neighbouring IEL, akin to tonic signaling that is proposed to sustain peripheral αβ T cell survival and/or competence[42]. Indeed, steady-state ligand engagement by HV4 may induce in in primary IEL different signaling events to those induced by ligand binding to CRDs1-3. In this regard, there is no evidence that Btnl/BTNL interactions determine peripheral clonal dominance; thus, fairly comparable responses to 293T.L3L8 cells were mediated by TCRs that were either highly abundant (e.g. hu12) or rare (e.g. hu7) in the deep sequencing data-set. Conceivably, tonic signaling of αβ T cells may also be a "neutral event" that does not influence clonal dominance.

Each of the clonally-restricted TCR antigens considered in this study is an MHC-related molecule. Although neither MHC nor CD1 molecules are required for γδ T cell repertoire development, their potential to function as clone-specific ligands is well established[18, 43]. Several such ligands have been considered "stress-antigens", promoting γδ T cell responses to dysregulated tissues, including cancer cells. Thus the γδ TCR might use HV4 to sense "normal self", and CDR1-3 to sense "stressed self", in which regard it is intriguing that Btnl/BTNL proteins are related to B7 proteins that communicate pathophysiologic contexts to regulate the responses of adaptive lymphocytes. In this context, the quasi-monomorphic DETC receptor may have a *Btnl*-like ligand at steady state (e.g. a Skint1 complex) and qualitatively distinct ligand(s) on dysregulated cells[44].

The apparently generalizable capacity of HV4 to form a solvent-exposed loop in γδTCRs raises the question as to whether it is broadly deployed to engage self-agonists. There is evidence for agonist selection of several γδ T cell subsets[45, 46], and HV4-mediated agonist selection might in paritcular underpin the development of

several tissue-associated γδ T cell compartments that are partly defined by restricted Vγ chain usage, and that effect different pre-programmed functions in response to myriad innate stimuli[18]. Moreover, in cases where TCR signaling promoted cell death in developing γδ T cells[47], it might be appropriate to evaluate whether this is also true for HV4-dependent signals.

Likewise, our findings may have implications for TCRαβ$^+$ NKT and MAIT cells which are partly defined by highly restricted TCRVα chain usage, and which undergo self-agonist selection prior to making rapid, polyclonal responses to innate stimuli, e.g. IL-12+IL-18. Whereas selection depends upon determinants, such as CD1d-lipid complexes that bind TCRαβ CDRs[48, 49, 50], the possible contribution(s) of HV4 may merit further study. Indeed, so-called "super-antigens", which can profoundly influence αβ T cell repertoire development, mediate their effects by engaging TCRVβ-specific FR3 residues, including HV4, that transduce qualitatively distinct signals from those induced by CDR1-3 engagement[51, 52, 53].

Similarly, there might be a role(s) of HV4 in the antigen receptors of B1 B cells whose repertoires are seemingly shaped by agonist selection events that also drive the cells' pre-programmed differentiation and association with non-lymphoid tissues[54]. FR3/HV4 residues of human Igs seem rarely to be implicated in foreign antigen binding, but were recently associated with high-affinity binding to auto-antigens in patients with central tolerance defects[55]. Possibly this reflects a generalisable capacity of HV4 regions to engage endogenous ligands in a growing number of pathophysiologic processes.

METHODS

Human samples

Human endoscopy biopsies were obtained from macroscopically healthy mucosa from the ascending colon of adult patients undergoing diagnostic colonoscopy after informed consent and in compliance with ethical approval (16/LO/0642) from the NHS Health Research Authority (London – Fulham Research Ethics Committee).

Mice

Wild-type (WT) C57Bl/6J mice were obtained from Jackson Laboratories and maintained at The Francis Crick Institute's Biological resource facilities. Male mice aged between 3 and 5 weeks were used in this study. Animal experiments were undertaken in full compliance with the UK Home Office regulations and under a project license (7009056) to A.C.H.

Isolation of primary IEL

Human colonic lymphocytes were isolated as previously described[22] and used after a 5-7 days culture period. Mouse IEL were isolated from small intestine as previously described[22].

Cell lines

HEK293T, HT29, CHO (ATCC) and MODE-K cells (a kind gift from Dr. D. Kaiserlian, INSERM U1111, Lyon, France) were maintained in DMEM supplemented with 4.5 g/L D-glucose, L-glutamine, 10% heat-inactivated fetal calf serum (FCS) and 1% penicillin/streptomycin (pen/strep). J76, E6.1 and PAM2.12 cells were maintained in RPMI 1640 L-glutamine, 10% heat-inactivated FCS, 1%

pen/Strep. All cell culture reagents were from Thermo Fisher. NFAT-Gaussia luciferase (Gluc) reporter cell line JRT3[31] was maintained in complete RPMI (above) supplemented with 0.5 mg/ml G418 (Sigma-Aldrich). For transgenic HEK293T, MODE-K, PAM2.12 and CHO cells, medium was supplemented with 1 μg/ml Puromycin (Sigma-Aldrich) and/or 500 μg/ml Hygromycin (Thermo Fisher).

Flow cytometry

Flow cytometry was performed using the following antibodies, coupled to the indicated fluorochromes. *Antibodies for mouse:* CD3ε-APC/Cy7 (145-2C11), γδTCR-PECy7 (GL3 from eBioscience), γδTCR- PerCPeFluor710 (GL3), γδTCR-PE (GL3), γδTCR-BV421 (GL3), Vγ3-BV421 (536 from BD Bioscience), Vγ3-APC (536), Vδ4-FITC (GL2), TCRβ-BV421 (H57-597), CD25-PerCP/Cy5.5 (PC61), CD122-PE (TM-β1), CD71-FITC (RI7217), Nur77-PerCPeFluor710 (12.14 from eBioscience). *Antibodies for human:* CD69-AF647 (FN50), CD69-PE (FN50), CD3-FITC (UCHT1), CD3-BV421 (OKT3), CD3-BV786 (OKT3), γδTCR-PeCy7 (IMMU510 from Beckman Coulter), Vδ1-APC (REA173 from Miltenyi), Vδ2-PerCpCy5.5 (B6), CD25-BV421 (BC96), CD45RA-PE (HI100). The Vγ2/3/4 biotin (23D12) antibody[32] was detected by conjugation to PE-Streptavidin. *Other antibodies:* DYKDDDDK-PE (Flag), DYKDDDDK-APC (Flag), HA-DyLight 650 (2-2.2.14, Invitrogen), HA-BV421 (16B12), HA-AF647 (16B12), EPCR-PE (RCR-16), EPCR-APC (RCR-16). Antibodies for flow were purchased from Biolegend unless otherwise stated; viability dies (Blue or Aqua) were from Invitrogen. Anti-TCRVγ7 producing hybridoma (F2.67) was kindly provided by Pablo Pereira (Institut Pasteur, Paris, France). The antibody was purified from hybridoma supernatant using the mouse TCS purification

system (abcam-ab128749) and conjugated to AF647 (labeling kit, Thermo Fisher Scientific).

Nur77 staining was performed on cells firstly fixed for 10' with CellFIX (BD Bioscience), then fixed and permeabilised using the Foxp3/Transcription factor staining buffer set (eBioscience). In one experiment, MODE-K cells were fixed for 10' with CellFIX and thoroughly rinsed prior to co-culture assay.

Flow cytometry data analysis was performed on FlowJo (Version 10).

CD1 protein production and CD1c-PC dextramers

Plasmids encoding the extracellular domains of human CD1c, and human β2-microglobulin (β2m) were separately cloned into the prokaryotic expression vector pET23d (Novagen). CD1c and β2m were subsequently produced as inclusion bodies in Escherichia coli Rosetta strain (Novagen). Inclusion bodies were thoroughly washed and fully denatured then reduced in 6 M guanidineHCl and 20 mM DTT before *in vitro* refolding. Refolding of CD1c/β2m complexes was performed by oxidative *in vitro* refolding as previously described[56] in the presence of Phosphatidylcholine (PC) (Avanti Polar Lipids). Correctly folded proteins were purified by size-exclusion chromatography using preparatory grade SD75 26/60 and analytical grade SD75 GL 10/300 gel filtration columns (GE Healthcare). Refolded CD1c-PC complexes were biotinylated via an engineered BirA motif at the C terminus, repurified by size exclusion chromatography before conjugation to dextran-PE (Immudex) to generate labelled CD1c-dextramers[31].

Co-culture assay

Co-cultures of murine primary IEL with MODE-K and primary human IEL with

293T were performed as described previously[22]. $0.5x10^5$ J76 transductants were cultured for 5 h on a confluent monolayer of MODE-K, 293T, CHO and PAM2.12 previously seeded in 48-well plates. Alternatively, $0.5x10^5$ J76, JRT3 NFAT-GLuc or E6.1 transductants were mixed in 96-well plates with either $2x10^5$ MODE-K or 293T and co-cultured for 5 h. As control, $0.5x10^5$ J76 cells were stimulated in 96-well plates with 10 μg/ml of α-CD3ε (OKT3) or, for the human TCRs, pan-γδTCR (B1), and Isotype control IgG (Biolegend). In EPCR blocking experiments, 293T cells were pre-incubated with 10 μg/mL α-EPCR or goat IgG (R&D Systems) for 45 min.

Single-cell PCR and sequencing

A 96-well plate of single cell-sorted responding cells ($CD122^{low}CD25^{high}$ in mouse and $TCR^{low}CD25^{high}$ in human) was thawed on ice, incubated at 65°C for 5min and placed back on ice. The reverse transcription and first round of PCR were performed using the qScript XLT One-Step RT-PCR Kit (Quanta Biosciences) following manufacturer's recommendations with slight modifications. External primers sets were used in a 20μL reaction (500nM total concentration for each forward and reverse sets). PCR products were then diluted 1:5 for a second round of PCR using internal sets of primers and Phusion High-Fidelity DNA Polymerase (NEB). Second round PCR products were ran on a 2% agarose gel, bands were excised and purified (QIAquick Gel Extraction Kit, Qiagen). Purified amplicons were sent for Sanger sequencing to Eurofins Genomics using custom primers. All primers referred to above are listed in Supplementary Table 2.

TCR deep sequencing

Human bulk mRNA was extracted from donor biopsies using AllPrep DNA/RNA Mini kit (Qiagen) and sent for γδTCR chain deep-sequencing using the IlluminaMiSeq platform with short-read 100/150 PER primers (iRepertoire, Huntsville, Alabama, USA). mRNA was extracted from bulk sorted $V\gamma7^+$ and $V\gamma7^-$ IEL using the RNA-Micro-plus kit (QIAGEN). Mouse *Trgv7* and *Trdv* genes deep-sequencing was performed as above.

Plasmids and cloning

Full-length gamma and delta chains were cloned into the self-inactivating lentiviral vector pCSIGPW[22, 23] after removal of the IRES-GFP and CMVp-$Puro^R$ cassettes. Overlap-extension PCR (OE-PCR) was used to replace CDR3 regions with AjuI and BaeI restriction sites. Final modified delta chains were subcloned using XhoI/NotI (for human constructs) and NcoI/XbaI (for mouse constructs); gamma chain was subcloned using NcoI/XbaI (for human constructs) and PmeI/NotI (for mouse constructs). Human Vγ9Vδ2 and mouse Vγ5Vδ1 pCSIW constructs were made with no restriction sites modifications. Paired CDR3γ/δ sequences were cloned using short annealed oligos. Plasmids coding for N-terminus-tagged Btnl/BTNL were described[23]. EPCR was cloned from HT29 cDNA into pCSIGPW using XhoI/NotI restriction sites. T22 was cloned from small intestine cDNA of a C57Bl/6 mouse into pCSIGPW using PmeI/NotI restriction sites. Mutations to swap CDR/HV4 regions or aminoacids (TCRs), solvent-exposed IgV-aminoacids (BTNL3/8) or to remove endogenous restriction sites by introduction of silent mutations were all performed by OE-PCR.

Lentiviral production and transduction

All plasmids used for lentiviral transductions were purified using a NucleoBond Xtra Midi EF kit (Macherey-Nagel). Lentiviral particles were produced in HEK293T cells by co-transfection of pCSIW encoding different TCRs, HIV-1 *gag-pol* pCR/V1[57], and VSV-G *env* pHIT/G[58]. Media was replaced 16 h post-transfection and collected at 48 h, filtered through 0.45μm nylon mesh and used to transduce 1-2.5x10^5 J76, E6.1 JRT3 NFAT-GLuc cells by spinoculation at 1,000 g for 30 min. Cells were assessed for TCR expression after 2-5 days. Adherent cell lines were transduced with the indicated combinations of FLAG-BTNL3, HA-BTNL8, HA-Btnl6, His-T22 and EPCR cloned into pCSIGPW, and FLAG-Btnl1 cloned into pCSIYHW. Viral supernatant supplemented with polybrene (1 μg/ml) was added to 50 % confluent cells plated 24h prior to transduction. 48h post-transduction, media was supplemented with appropriate concentration of antibiotics (Hygromycin and/or Puromycin) and when necessary, cells were sorted based on GFP and/or Tag expression.

Co-immunoprecipitation and Mass spectrometry

Lysates of MODE-K cells transduced with an empty vector (EV) control or with *Btnl1*-FLAG and *Btnl6*-HA were incubated with anti-DYKDDDDK magnetic agarose beads, followed by protein elution and SDS/PAGE. Anti-FLAG immunoprecipitation and mass spectrometry analysis were performed as previously described[23].

Western blot

Cell lines were kept overnight in starving media (SM, RPMI 0.5% FBS) harvested, washed with SM and allowed to rest in suspension for 1 h at 37°C, 5% CO_2. 2.5x10^5 JRT3-LES cells were mixed with 6.25x10^5 stimulatory cells; or 10 μg/mL α-CD3ε

(UCHT1) and 10 μg/mL pan-γδTCR (B1) crosslinked with anti-mouse IgG (Biolegend). Cells were spun down at 600 g for 1 min and incubated at 37˚C. 1 mL ice-cold PBS was then added at 5, 10 and 20 min, and spun down 600g, 2min, 4˚C. $2.5x10^5$ J76-*mo8* cells were mixed with $5x10^5$ MODE-K expressing empty vector, l1l6 and/or T22; or 10 μg/ml OKT3, UCHT1 and pan-γδTCR (GL3) crosslinked with anti-mouse/hamster IgG (Biolegend and Vector laboratories, respectively). Cells were spun down at 600 g for 1 min and incubated for 10 min at 37˚C. Pellets were then re-suspended in 100 μl ice-cold lysis buffer (50 mM Tris, pH 8, 150 mM NaCl, 0.5% NP-40, Protease and Phosphatase Inhibitor Cocktail [ThermoFisher]). Lysates were incubated for 20 min on ice and spun at 20,000 g for 20 min at 4˚C. Supernatants were then mixed with NuPAGE LDS Sample Buffer supplemented with β2-Mercaptenol (2.5% final concentration) or with 50mM DTT, loaded onto NuPAGE 4-12% Bis-Tris protein gels (ThermoFisher) and transferred onto nitrocellulose membranes. Membranes were then incubated in blocking solution (PBS/TBS, 0.1% Tween20, 3% BSA) for 90 min at room temperature and subsequently with primary antibodies (1:1000 dilution in blocking solution) overnight at 4˚C. Membranes were then washed in PBS/TBS 0.1% Tween20, incubated for 1 hour at room temperature with secondary antibodies (1:5000 dilution in blocking solution), washed again and developed with Clarity Max Western ECL Blotting Substrate (BioRad) or with ECL Western Blotting Detection Reagents (GE Healthcare). Anti CD3ε (#4443), Phospho-LAT (Tyr191) (#3584), Phospho-PLCγ1 (Tyr783) (#14008/2821), HRP-linked anti-rat IgG (#7077), HRP-linked anti-rabbit IgG (#7074) and HRP-linked anti-mouse IgG (#7076) antibodies were from Cell Signalling Technologies. Anti CD247 (51-6527GR) antibody was purchased from BD.

Luciferase assay

The JRT3 NFAT-Gluc reporter cell line[31] was transduced with γδTCRs and $2x10^5$ cells were co-cultured with $5x10^5$ 293T expressing EV or L3L8, or with MODE-K expressing EV or l1l6 at 37˚C, 5% CO_2. Alternatively, JRT3 lines were stimulated with 10 ng/ml PMA (phorbol 12-myristate 13-acetate) and 1 μg/ml ionomycin. After 24h, supernatants were collected and luciferase activity was measured using the BioLux Gaussia Luciferase Assay Kit (NEB) following the manufacturer's instructions. Luminescence was acquired on an EnVision plate-reader (PerkinElmer). Background levels were measured from untransduced reporter cell lines.

ELISA assay

E6.1 cells were transduced with murine γδTCRs and $5x10^4$ cells were co-cultured with $2x10^5$ MODE-K expressing EV or l1l6 at 37°C for 24 hours. As control, E6.1 cells were stimulated with 1 μg/ml of α–CD3ε (OKT3) or IgG2a soluble antibodies. After 24h, supernatants were collected and secreted IL-2 was measured using the Elisa Max Kit (Biolegend) following the manufacturer's instructions. 450nm absorbance was measured on an Infinite 200 PRO (Tecan) plate reader.

RNAscope

RNAscope was performed on paraffin embedded sections using probes and kits obtained from Advanced Cell Diagnostics using the RNAscope 2.5 HD Duplex Assay-RED (performed as single-plex). Probe HS-TRDC-C2 (#433671-C2) was used to detected TCRδ chain mRNA. RNAscope. Positive Control Probe - Hs-PPIB-C2 (#313901-C2). RNAscope Negative Control Probe - Hs-dapB (#310043).

Soluble recombinant TCR

Soluble γδ TCR heterodimers constructs were generated by fusing γ and δ variable domains to β and α constant domains respectively, with a C-terminal addition of the heterodimerization motifs Acid-p1 and Base-p1[59], respectively. A 6xHis-tag was added to the resulting δ-α-Base-p1 chain to allow detection using an APC-α-His antibody. The CDR3 sequence used for all γ chain constructs was from the Dp10.7 TCR[7]. The CDR3 sequence used for both the Vδ1 and Vδ2 constructs was from the d1A/B-3 TCR[60]. Heterodimers were expressed in HEK293 cells and purified using size exclusion-high-performance liquid chromatography (SEC-HPLC). All constructs were produced and purified by Iontas (Cambridge, UK).

Modelling software code availability

3D-JIGSAW and SwarmDock were used to generate 3D models of proteins and perform docking simulations, respectively. The full source codes have not been released. Publicly available servers for 3D-JIGSAW and SwarmDock can be accessed at https://bmm.crick.ac.uk/~svc-bmm-3djigsaw/ and https://bmm.crick.ac.uk/~svc-bmm-swarmdock/index.html respectively.

Statistical analysis

GraphPad Prism (version 7) was used to perform statistical analysis. *P* values were determined by paired two-tailed Student's *t*-tests. *n* values and error bars are defined in each figure legend.

Reporting Summary

Additional information on study design and reagents is available in the Reporting Summary linked to this article.

Data availability

This work did not include any data with mandated deposition in public databases. Associated raw data are provided in the main and/or supplementary figures. Relations to summary data charts are indicated and a full list of figures with associated raw data is provided in the Reporting Summary linked to this article.

ACKNOWLEDGEMENTS

We are grateful to C. Willcox, B. Willcox (University of Birmingham), and P. Barral (The Francis Crick Institute) for cell lines; R.P. Di Marco Barros (UCL), A. Jandke (FCI), A. Lorrenc, D. Ushakov and A. Laing (FCI&KCL) for contributions and discussions; E. Theodoridis (KCL), the flow cytometry, genomic equipment park, bio-informatics, experimental histopathology, mass spectrometry and proteomics platform, cell services, and biological service units of the FCI, the Peter Gorer Department of Immunobiology and the Guy's Hospital Biomedical Research Centre (BRC) for outstanding technical support; and the NVIDIA corporation for the donation of a Titan Xp GPU used to run our protein-protein docking algorithm. The work was supported by the FCI, which receives its core funding from Cancer Research UK (FC001003), the UK Medical Research Council (FC001003), and the Wellcome Trust (FC001003); studentships from the King's King's Bioscience Institute and the Guy's and St. Thomas' Charity Prize PhD program in Biomedical and Translational Science (D.M.), the National Institute for Health Research (NIHR)

Biomedical Research Centre at Guy's and St Thomas' NHS Foundation Trust and King's College London [to I.Z.], and the Wellcome Trust (108745/Z/15/Z) (R.J.D); funds from St. Thomas' Wegener's Trust and MRC (MR/P021964/1) (S.J.), the Cluster of Excellence ExC 306 "Inflammation-at-Interfaces" (D.W. and D.K.), Cancer Research UK (23562) (S.M), and the Wellcome Trust (106292/Z/14/Z and 100156/Z/12/Z) (A.C.H).

COMPETING INTERESTS STATEMENT

O.N. and O.P. are employees of GammdaDelta Therapeutics. O.N., O.P., and A.H.C. are equity holders in GammaDelta Therapeutics.

AUTHOR CONTRIBUTIONS

D.M., I.Z., R.A.G.C., R.J.D., N.A.R., S.J., and P.V. designed and undertook experiments; O.N., O.P., D.W., D.K., A.C. and S.M. designed, prepared and provided critical reagents, D.M., I.Z., R.A.G.C., R.D., N.R., P.M.I., S.J., S.M., P.A.B., P.V. and A.C.H. processed and interpreted data; D.M., I.Z., R.J.D., and N.A.R revised the manuscript; P.V. and A.H. designed the study and wrote the manuscript.

DEDICATION

This manuscript is dedicated to the memory of Dr. Bruno Kyewski who greatly clarified our insights into T cell tolerance and selection.

REFERENCES

1. Hayday, A.C. [gamma][delta] cells: a right time and a right place for a conserved third way of protection. *Annu Rev Immunol* **18**, 975-1026 (2000).

2. Davey, M.S. *et al.* The human Vdelta2(+) T-cell compartment comprises distinct innate-like Vgamma9(+) and adaptive Vgamma9(-) subsets. *Nat Commun* **9**, 1760 (2018).

3. Davey, M.S. *et al.* Clonal selection in the human Vdelta1 T cell repertoire indicates gammadelta TCR-dependent adaptive immune surveillance. *Nat Commun* **8**, 14760 (2017).

4. Ravens, S. *et al.* Human gammadelta T cells are quickly reconstituted after stem-cell transplantation and show adaptive clonal expansion in response to viral infection. *Nat Immunol* **18**, 393-401 (2017).

5. Gober, H.J. *et al.* Human T cell receptor gammadelta cells recognize endogenous mevalonate metabolites in tumor cells. *J Exp Med* **197**, 163-168 (2003).

6. Adams, E.J., Chien, Y.H. & Garcia, K.C. Structure of a gammadelta T cell receptor in complex with the nonclassical MHC T22. *Science* **308**, 227-231 (2005).

7. Luoma, A.M. *et al.* Crystal structure of Vdelta1 T cell receptor in complex with CD1d-sulfatide shows MHC-like recognition of a self-lipid by human gammadelta T cells. *Immunity* **39**, 1032-1042 (2013).

8. Willcox, C.R. *et al.* Cytomegalovirus and tumor stress surveillance by binding of a human gammadelta T cell antigen receptor to endothelial protein C receptor. *Nat Immunol* **13**, 872-879 (2012).

9. Groh, V., Steinle, A., Bauer, S. & Spies, T. Recognition of stress-induced MHC molecules by intestinal epithelial gammadelta T cells. *Science* **279**, 1737-1740 (1998).

10. Marlin, R. *et al.* Sensing of cell stress by human gammadelta TCR-dependent recognition of annexin A2. *Proc Natl Acad Sci U S A* **114**, 3163-3168 (2017).

11. Bruder, J. *et al.* Target specificity of an autoreactive pathogenic human gammadelta-T cell receptor in myositis. *J Biol Chem* **287**, 20986-20995 (2012).

12. Asarnow, D.M. *et al.* Limited diversity of gamma delta antigen receptor genes of Thy-1+ dendritic epidermal cells. *Cell* **55**, 837-847 (1988).

13. Havran, W.L., Carbone, A. & Allison, J.P. Murine T cells with invariant gamma delta antigen receptors: origin, repertoire, and specificity. *Semin Immunol* **3**, 89-97 (1991).

14. Kyes, S., Carew, E., Carding, S.R., Janeway, C.A., Jr. & Hayday, A. Diversity in T-cell receptor gamma gene usage in intestinal epithelium. *Proc Natl Acad Sci U S A* **86**, 5527-5531 (1989).

15. Hayday, A.C. Gammadelta T cells and the lymphoid stress-surveillance response. *Immunity* **31**, 184-196 (2009).

16. Medzhitov, R. & Janeway, C.A., Jr. Innate immunity: the virtues of a nonclonal system of recognition. *Cell* **91**, 295-298 (1997).

17. Strid, J. *et al.* Acute upregulation of an NKG2D ligand promotes rapid reorganization of a local immune compartment with pleiotropic effects on carcinogenesis. *Nat Immunol* **9**, 146-154 (2008).

18. Vantourout, P. & Hayday, A. Six-of-the-best: unique contributions of gammadelta T cells to immunology. *Nat Rev Immunol* **13**, 88-100 (2013).

19. Leishman, A.J. *et al.* Precursors of functional MHC class I- or class II-restricted CD8alphaalpha(+) T cells are positively selected in the thymus by agonist self-peptides. *Immunity* **16**, 355-364 (2002).

20. Boyden, L.M. *et al.* Skint1, the prototype of a newly identified immunoglobulin superfamily gene cluster, positively selects epidermal gammadelta T cells. *Nat Genet* **40**, 656-662 (2008).

21. Turchinovich, G. & Hayday, A.C. Skint-1 identifies a common molecular mechanism for the development of interferon-gamma-secreting versus interleukin-17-secreting gammadelta T cells. *Immunity* **35**, 59-68 (2011).

22. Di Marco Barros, R. *et al.* Epithelia Use Butyrophilin-like Molecules to Shape Organ-Specific gammadelta T Cell Compartments. *Cell* **167**, 203-218 e217 (2016).

23. Vantourout, P. *et al.* Heteromeric interactions regulate butyrophilin (BTN) and BTN-like molecules governing gammadelta T cell biology. *Proc Natl Acad Sci U S A* **115**, 1039-1044 (2018).

24. Salim, M. *et al.* Characterization of a Putative Receptor Binding Surface on Skint-1, a Critical Determinant of Dendritic Epidermal T Cell Selection. *J Biol Chem* **291**, 9310-9321 (2016).

25. Harly, C. *et al.* Key implication of CD277/butyrophilin-3 (BTN3A) in cellular stress sensing by a major human gammadelta T-cell subset. *Blood* **120**, 2269-2279 (2012).

26. Kisielow, J., Tortola, L., Weber, J., Karjalainen, K. & Kopf, M. Evidence for the divergence of innate and adaptive T-cell precursors before commitment to the alphabeta and gammadelta lineages. *Blood* **118**, 6591-6600 (2011).

27. Goodman, T. & Lefrancois, L. Intraepithelial lymphocytes. Anatomical site, not T cell receptor form, dictates phenotype and function. *J Exp Med* **170**, 1569-1581 (1989).

28. San Jose, E., Borroto, A., Niedergang, F., Alcover, A. & Alarcon, B. Triggering the TCR complex causes the downregulation of nonengaged receptors by a signal transduction-dependent mechanism. *Immunity* **12**, 161-170 (2000).

29. Heemskerk, M.H. *et al.* Redirection of antileukemic reactivity of peripheral T lymphocytes using gene transfer of minor histocompatibility antigen HA-2-specific T-cell receptor complexes expressing a conserved alpha joining region. *Blood* **102**, 3530-3540 (2003).

30. Moran, A.E. *et al.* T cell receptor signal strength in Treg and iNKT cell development demonstrated by a novel fluorescent reporter mouse. *J Exp Med* **208**, 1279-1289 (2011).

31. Chancellor, A. *et al.* CD1b-restricted GEM T cell responses are modulated by Mycobacterium tuberculosis mycolic acid meromycolate chains. *Proc Natl Acad Sci U S A* **114**, E10956-E10964 (2017).

32. Kabelitz, D. *et al.* New monoclonal antibody (23D12) recognizing three different V gamma elements of the human gamma delta T cell receptor. 23D12+ cells comprise a major subpopulation of gamma delta T cells in postnatal thymus. *J Immunol* **152**, 3128-3136 (1994).

33. Hayes, S.M., Shores, E.W. & Love, P.E. An architectural perspective on signaling by the pre-, alphabeta and gammadelta T cell receptors. *Immunol Rev* **191**, 28-37 (2003).

34. Palakodeti, A. *et al.* The molecular basis for modulation of human Vgamma9Vdelta2 T cell responses by CD277/butyrophilin-3 (BTN3A)-specific antibodies. *J Biol Chem* **287**, 32780-32790 (2012).

35. Bates, P.A., Kelley, L.A., MacCallum, R.M. & Sternberg, M.J. Enhancement of protein modeling by human intervention in applying the automatic programs 3D-JIGSAW and 3D-PSSM. *Proteins* **Suppl 5**, 39-46 (2001).

36. Torchala, M., Moal, I.H., Chaleil, R.A., Fernandez-Recio, J. & Bates, P.A. SwarmDock: a server for flexible protein-protein docking. *Bioinformatics* **29**, 807-809 (2013).

37. Holness, C.L. & Simmons, D.L. Structural motifs for recognition and adhesion in members of the immunoglobulin superfamily. *J Cell Sci* **107 (Pt 8)**, 2065-2070 (1994).

38. Green, N. *et al.* Mutational analysis of MAdCAM-1/alpha4beta7 interactions reveals significant binding determinants in both the first and second immunuglobulin domains. *Cell Adhes Commun* **7**, 167-181 (1999).

39. Jones, E.Y. *et al.* Crystal structure of an integrin-binding fragment of vascular cell adhesion molecule-1 at 1.8 A resolution. *Nature* **373**, 539-544 (1995).

40. Moebius, U., Pallai, P., Harrison, S.C. & Reinherz, E.L. Delineation of an extended surface contact area on human CD4 involved in class II major histocompatibility complex binding. *Proc Natl Acad Sci U S A* **90**, 8259-8263 (1993).

41. Somoza, C., Driscoll, P.C., Cyster, J.G. & Williams, A.F. Mutational analysis of the CD2/CD58 interaction: the binding site for CD58 lies on one face of the first domain of human CD2. *J Exp Med* **178**, 549-558 (1993).

42. Myers, D.R., Zikherman, J. & Roose, J.P. Tonic Signals: Why Do Lymphocytes Bother? *Trends Immunol* **38**, 844-857 (2017).

43. Hayday, A. & Vantourout, P. A long-playing CD about the gammadelta TCR repertoire. *Immunity* **39**, 994-996 (2013).

44. Komori, H.K. *et al.* Cutting edge: dendritic epidermal gammadelta T cell ligands are rapidly and locally expressed by keratinocytes following cutaneous wounding. *J Immunol* **188**, 2972-2976 (2012).

45. Fahl, S.P. *et al.* Role of a selecting ligand in shaping the murine gammadelta-TCR repertoire. *Proc Natl Acad Sci U S A* **115**, 1889-1894 (2018).

46. Wencker, M. *et al.* Innate-like T cells straddle innate and adaptive immunity by altering antigen-receptor responsiveness. *Nat Immunol* **15**, 80-87 (2014).

47. Sumaria, N., Grandjean, C.L., Silva-Santos, B. & Pennington, D.J. Strong TCRgammadelta Signaling Prohibits Thymic Development of IL-17A-Secreting gammadelta T Cells. *Cell Rep* **19**, 2469-2476 (2017).

48. Cernadas, M. *et al.* Lysosomal localization of murine CD1d mediated by AP-3 is necessary for NK T cell development. *J Immunol* **171**, 4149-4155 (2003).

49. Chiu, Y.H. *et al.* Multiple defects in antigen presentation and T cell development by mice expressing cytoplasmic tail-truncated CD1d. *Nat Immunol* **3**, 55-60 (2002).

50. Mallevaey, T. *et al.* T cell receptor CDR2 beta and CDR3 beta loops collaborate functionally to shape the iNKT cell repertoire. *Immunity* **31**, 60-71 (2009).

51. Bueno, C. *et al.* Bacterial superantigens bypass Lck-dependent T cell receptor signaling by activating a Galpha11-dependent, PLC-beta-mediated pathway. *Immunity* **25**, 67-78 (2006).

52. Fields, B.A. *et al.* Crystal structure of a T-cell receptor beta-chain complexed with a superantigen. *Nature* **384**, 188-192 (1996).

53. Kreiss, M. *et al.* Contrasting contributions of complementarity-determining region 2 and hypervariable region 4 of rat BV8S2+ (Vbeta8.2) TCR to the recognition of myelin basic protein and different types of bacterial superantigens. *Int Immunol* **16**, 655-663 (2004).

54. Hayakawa, K. *et al.* Positive selection of natural autoreactive B cells. *Science* **285**, 113-116 (1999).

55. Meyer, S. *et al.* AIRE-Deficient Patients Harbor Unique High-Affinity Disease-Ameliorating Autoantibodies. *Cell* **166**, 582-595 (2016).

56. Mansour, S. *et al.* Cholesteryl esters stabilize human CD1c conformations for recognition by self-reactive T cells. *Proc Natl Acad Sci U S A* **113**, E1266-1275 (2016).

57. Zennou, V., Perez-Caballero, D., Gottlinger, H. & Bieniasz, P.D. APOBEC3G incorporation into human immunodeficiency virus type 1 particles. *J Virol* **78**, 12058-12061 (2004).

58. Fouchier, R.A., Meyer, B.E., Simon, J.H., Fischer, U. & Malim, M.H. HIV-1 infection of non-dividing cells: evidence that the amino-terminal basic region of the viral matrix protein is important for Gag processing but not for post-entry nuclear import. *EMBO J* **16**, 4531-4539 (1997).

59. O'Shea, E.K., Lumb, K.J. & Kim, P.S. Peptide 'Velcro': design of a heterodimeric coiled coil. *Curr Biol* **3**, 658-667 (1993).

60. Xu, B. *et al.* Crystal structure of a gammadelta T-cell receptor specific for the human MHC class I homolog MICA. *Proc Natl Acad Sci U S A* **108**, 2414-2419 (2011).

FIGURE LEGENDS

Figure 1. Primary Vγ7$^+$ IEL exhibit a semi-invariant TCR usage.

a, TCR deep-sequencing analysis of Vγ7 CDR3 length distribution (number of amino acids) of sorted Vγ7$^+$ cell RNA. Data are expressed as the relative proportion of reads for each length, pooled from three independent sorts from pooled mice IEL (n = 12). Relative amino acid composition is shown for the most common length (13) using WebLogo (black, hydrophobic; green, basic; red, acidic; blue, polar). **b,** TCR deep-sequencing data from (a) analysed to determine *Trdv* gene usage by Vγ7$^+$ cells. Data derived from Vγ7$^+$ cells sorted from pooled mice IEL (n = 4). Representative of three independent sorts. **c,** TCR deep-sequencing data from (a) was further analysed to determine Vδ7, Vδ2-2, and Vδ6D-1/2 CDR3 length distribution and composition for the most common length (16, 16 and 13, respectively), as in (a). **d,** Flow cytometry analysis of CD25 (left) and CD122 (centre) expression by primary Vγ7$^+$ IEL after co-culture with MODE-K.EV or MODE-K.l1l6 cells overnight. Data expressed as mean±s.d. of the proportion of positive Vγ7$^+$ IEL (CD25) or gMFI of Vγ7$^+$ IEL (CD122) in individual co-cultures (n = 4). Corresponding examples of raw flow cytometry plots are shown (right). Representative of five experiments. **e**,**f,** Flow cytometry analysis of CD3 (e) and CD71 (f) expression by Vγ7$^+$ IEL after co-culture with MODE-K.EV or .l1l6 cells. Data expressed as mean±s.d. of gMFI in co-cultures from individual mice (n = 4). Corresponding examples of raw flow cytometry plots are shown (right). Representative of five (CD3) and two (CD71) experiments. *P < 0.05, **P < 0.001.

Figure 2. Expression of murine Vγ7 TCR confers responsiveness to *Btnl1+Btnl6.*

a, Flow cytometry analysis of γδTCR, and Vγ7 or Vγ5 expression on J76 cells transduced with the indicated TCRs, 72 h post-transduction. Representative of 2 independent transductions. **b**, Flow cytometry analysis of γδTCR and CD69 expression by J76 cells transduced with the indicated TCRs and co-cultured with control IgG, α-CD3e (OKT3), MODE-K.EV, or MODE-K.l1l6 for 5 h. Representative of three independent experiments. **c,** Flow cytometry analysis of TCR downregulation (left) and CD69 upregulation (right) by J76 cells transduced with the indicated TCRs (see Table 1 for details) and co-cultured with MODE-K.l1l6 or α-CD3ε for 5 h. Data expressed as mean±s.d., normalized to MODE-K.EV and control IgG, respectively; pooled from three independent experiments. **d,** Flow cytometry analysis of Nur77 expression (left) by J76-mo5 cells co-cultured with the indicated antibodies or cell lines for 2 h. Data expressed as mean±s.d. of the proportion of $Nur77^+$ cells; pooled from three experiments. Corresponding examples of raw flow cytometry contour plots are shown (right). $*P < 0.05$, $**P < 0.01$, $***P < 0.001$.

Figure 3. Expression of human Vγ4 TCR confers responsiveness to *BTNL3+BTNL8.*

a, RNAscope analysis of TCRδ (*TRDC*, left), dihydropicolinate reductase (*dapB*, centre; negative control), or Peptidyl-prolyl Isomerase B (*PPIB*, bottom; positive control) expression in paraffin-embedded human colon sections. Scale bars, 1 mm. Representative of biopsies from multiple donors ($n = 3$). **b,** Flow cytometry analysis of TCR downregulation (top) and CD25 expression (bottom) by human colonic lymphocytes after co-culture with 293T.EV or 293T.L3L8 cells overnight. TCR downregulation data expressed as mean±s.d. of independent co-cultures from multiple

donors (n = 11) with 293T.L3L8 cells, normalized to 293T.EV cells. CD25 data shown as the paired proportion of $CD25^+$ cells within $V\gamma2/3/4^+$ cells in lymphocytes co-cultured with the indicated cell lines for each donor (n = 11). *P < 0.05, **P < 0.0001. **c,** Flow cytometry analysis of Vγ2/3/4 and γδTCR (donor 1), or Vγ2/3/4 and CD25 (donors 2 and 3) expression by human colonic lymphocytes after co-culture with the indicated cell lines overnight. Gates used for single-cell sorting are shown. Pre-gated on singlets/live/$CD3^+V\delta2^-/\gamma\delta TCR^+$ cells. **d,** Flow cytometry analysis of γδTCR and CD69 expression by J76-hu17 cells (see Table 2 for details) and co-cultured with the indicated antibodies or cell lines for 5 h. Representative of three independent experiments. **e,** Flow cytometry analysis of TCR downregulation (left) and CD69 upregulation (right) by J76 cells transduced with the indicated TCRs (see Table 2) and co-cultured with 293T.L3L8 or α-CD3ε (OKT3) for 5 h. Data expressed as mean±s.d. of individual co-cultures (n = 3), normalized to 293T.EV and control IgG respectively. Representative of three independent experiments.

Figure 4. Human $V\gamma4^{HV4}$ is a critical determinant of the response to BTNL3+8.

a, Alignment of human TCR Vγ chain amino acid sequences (divergence from Vγ4 in red). Variable regions are highlighted (green, CDR1; yellow, CDR2; pink, HV4; blue, CDR3). Horizontal arrow delineates Framework Region 3 (FR3). **b,c,d,** Flow cytometry analysis of TCR downregulation (x-axis) and CD69 upregulation (y-axis) by J76 cells transduced with hu17 or the indicated variants (see Supplementary Fig. 4a,b,c,d) and co-cultured with 293T.L3L8 for 5 h. Data expressed as mean±s.d. of individual co-cultures (n = 3), normalized to 293T.EV. Representative of two (b), three (c) and four (d) independent experiments.

Figure 5. Cross-species conservation of the critical role of HV4γ in the response to Btnl/BTNL.

a, Alignment of mouse Vγ7 and Vγ6 sequences (top), and of mo5 variants (bottom, differences from wild-type Vγ7 sequence in red). Due to space constraints the most C-terminal region sequence (YYCASWA, identical between all constructs), is not depicted. CDR1/2/3 regions are highlighted in green, yellow and cyan, respectively. **b,c,** Flow cytometry analysis of TCR downregulation (x-axis) and CD69 upregulation (y-axis) by J76 cells transduced with mo5 or the indicated variants (see Supplementary Fig. 5a,b,c,d) and co-cultured with MODE-K.l1l6 for 5 h. Data expressed as mean±s.d. of individual co-cultures (n = 3), normalized to MODE-K.EV. Representative of four independent experiments. **d,** Flow cytometry analysis of TCR downregulation (left) and CD69 upregulation (centre) by J76 cells transduced with the indicated TCRs and co-cultured with 293T.l1l6 or 293T.L3L8 for 5 h. Data expressed as mean±s.d. of individual co-cultures (n = 3), normalized to 293T.EV. Corresponding raw flow cytometry plots are shown (right). Representative of four independent experiments. *$P < 0.01$, **$P < 0.001$.

Figure 6. A proposed model for BTNL3 engagement by Vγ4$^+$ TCRs.

a, Flow cytometry analysis of TCR downregulation (top) and CD69 upregulation (bottom) by J76-hu17 co-cultured with the indicated stimulants. Data expressed as mean±s.d. of individual co-cultures (n = 3), normalized to 293T.EV. Representative of three independent experiments. **b,** Heterodimeric model of BTNL3 (green) / BTNL8 (teal), derived with 3D-JIGSAW from a BTN3A1 homodimer (PDB 4F80). Candidate motifs (see Supplementary Fig. 6c,d) are highlighted in orange, yellow, blue and red. **c,** Flow cytometry analysis of TCR downregulation (top) and CD69

upregulation (bottom) by J76-hu17 cells co-cultured with the indicated 293T transfectants for 5 h. Data expressed as mean±s.d. of individual co-cultures (n = 3), normalized to EV. Representative of three independent experiments. **d**, SwarmDock best-fit of TCR Vγ4 V-domain (light grey, PDB 4MNG) docking to BTNL3 IgV-domain (green). Motifs validated by functional assays (see Fig. 4c; Fig. 6c) are highlighted (TCR Vγ4: pink [HV4γ]; BTNL3: orange [NQFHA], blue [WF], red [DEEAT]) with side-chains displayed. **e**, Flow cytometry analysis of the indicated soluble TCRs (sTCR; pre-incubated with α-His antibody) binding to 293T.EV or 293T.L3L8 cells after incubation at 4˚C for 1 h. Representative of three independent experiments. **f,** Flow cytometry analysis of the indicated sTCR+α-His stainings. Data expressed as gMFI mean±s.d. of individual stainings (n = 3), normalized to α-His alone. **g,** Flow cytometry analysis of TCR downregulation (top) and CD69 upregulation (bottom) by J76-mo5 co-cultured with the indicated 293T transfectants for 5 h. Data expressed as mean±s.d. of individual co-cultures (n = 3), normalized to empty vector transfectants. Representative of three independent experiments.

Figure 7. Human Vγ4$^+$ and mouse Vγ7$^+$ TCRs exhibit dual-reactivity.

a, SwarmDock model showing the crystal structure of a Vγ4Vδ1 TCR binding CD1d-sulfatide (PDB 4MNG) docking to the complete BTNL3/BTNL8 heterodimer model (Fig. 6b). The docking solution is derived from Fig. 6d. **b,** Flow cytometry analysis of TCR downregulation (left) and CD69 upregulation (right) by JRT3 cells transduced with LES or hu12 TCRs and co-cultured with the indicated cell lines or α-CD3ε (OKT3) for 5 h. Data expressed as mean±s.d. of individual co-cultures (n = 3), normalized to 293T.EV or control IgG respectively. Representative of two independent experiments. **c,** Flow cytometry analysis of CD3ε and γδTCR expression

(left), and staining with Streptavidin alone (center) or pre-incubated with CD1c-PC (right) on J76 cells transduced with hu17 or hu20 TCRs. Representative of three experiments. **d,** Flow cytometry analysis of TCR downregulation (left) and CD69 upregulation (right) by J76 cells transduced with hu17 or hu20 TCRs and co-cultured with 293T.L3L8 cells or α-CD3ε for 5 h. Data expressed as mean±s.d. of individual co-cultures (n = 3), normalized to 293T.EV or control IgG, respectively. Representative of three independent experiments. **e,** Flow cytometry analysis of TCR downregulation (left) and CD69 upregulation (right) by J76 cells transduced with the mo8 (T22-specific) or mo5 (control) $V\gamma7^+$ TCRs and co-cultured with the indicated cell lines for 5 h. Data expressed as mean±s.d. (n = 3), normalized to MODE-K.EV or 293T.EV. Representative of five independent experiments. *$P < 0.05$, **$P < 0.01$, ***$P < 0.001$.

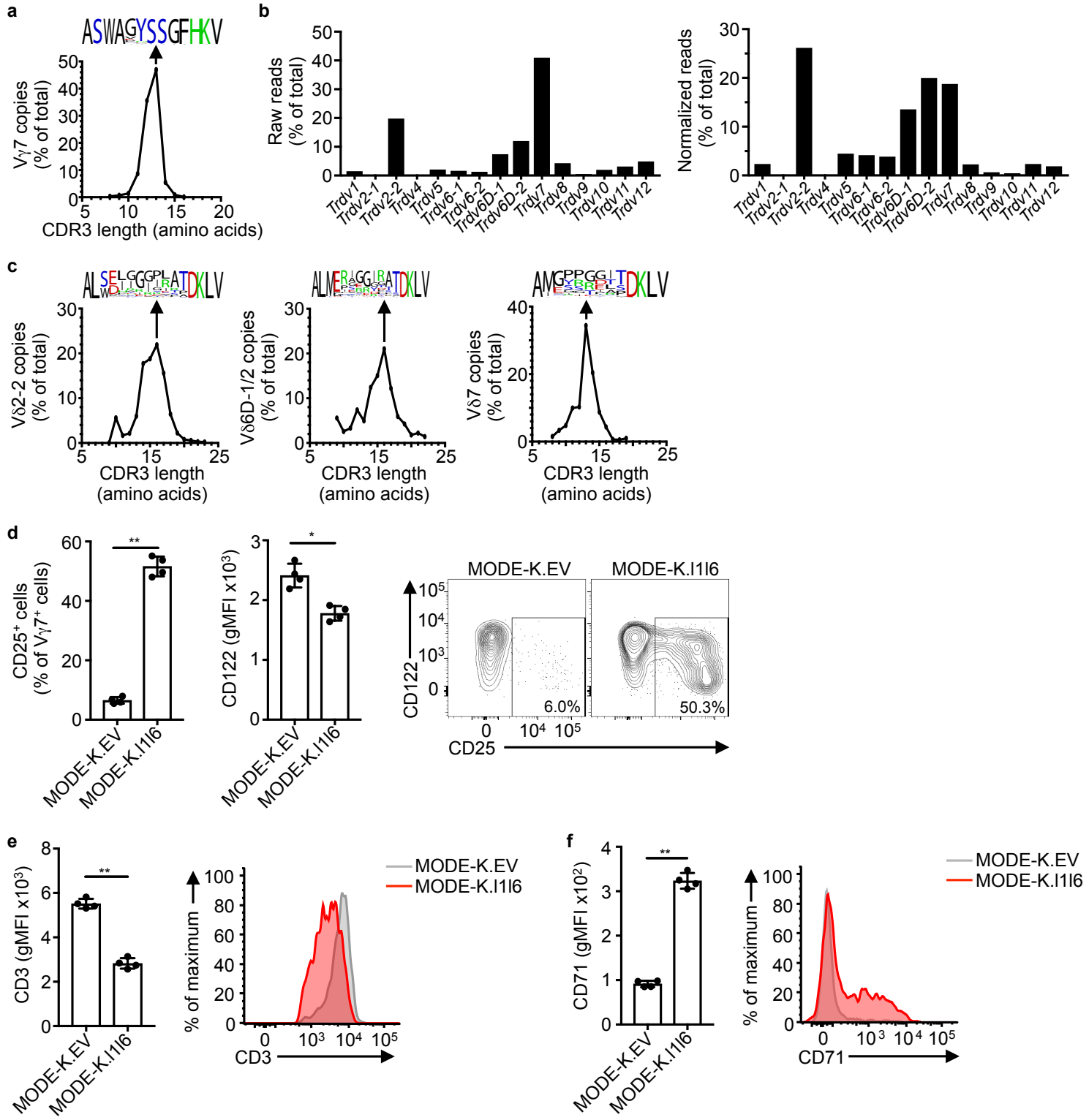
a
ASWAGYSSGFHKV
Vγ7 copies (% of total)
CDR3 length (amino acids)
b
Raw reads (% of total)
Normalized reads (% of total)
Trdv1
Trdv2-1
Trdv2-2
Trdv4
Trdv5
Trdv6-1
Trdv6-2
Trdv6D-1
Trdv6D-2
Trdv7
Trdv8
Trdv9
Trdv10
Trdv11
Trdv12
c
Vδ2-2 copies (% of total)
Vδ6D-1/2 copies (% of total)
Vδ7 copies (% of total)
CDR3 length (amino acids)
d
CD25+ cells (% of Vγ7+ cells)
CD122 (gMFI x10³)
MODE-K.EV
MODE-K.I1I6
6.0%
50.3%
CD122
CD25
e
CD3 (gMFI x10³)
% of maximum
CD3
f
CD71 (gMFI x10²)
CD71

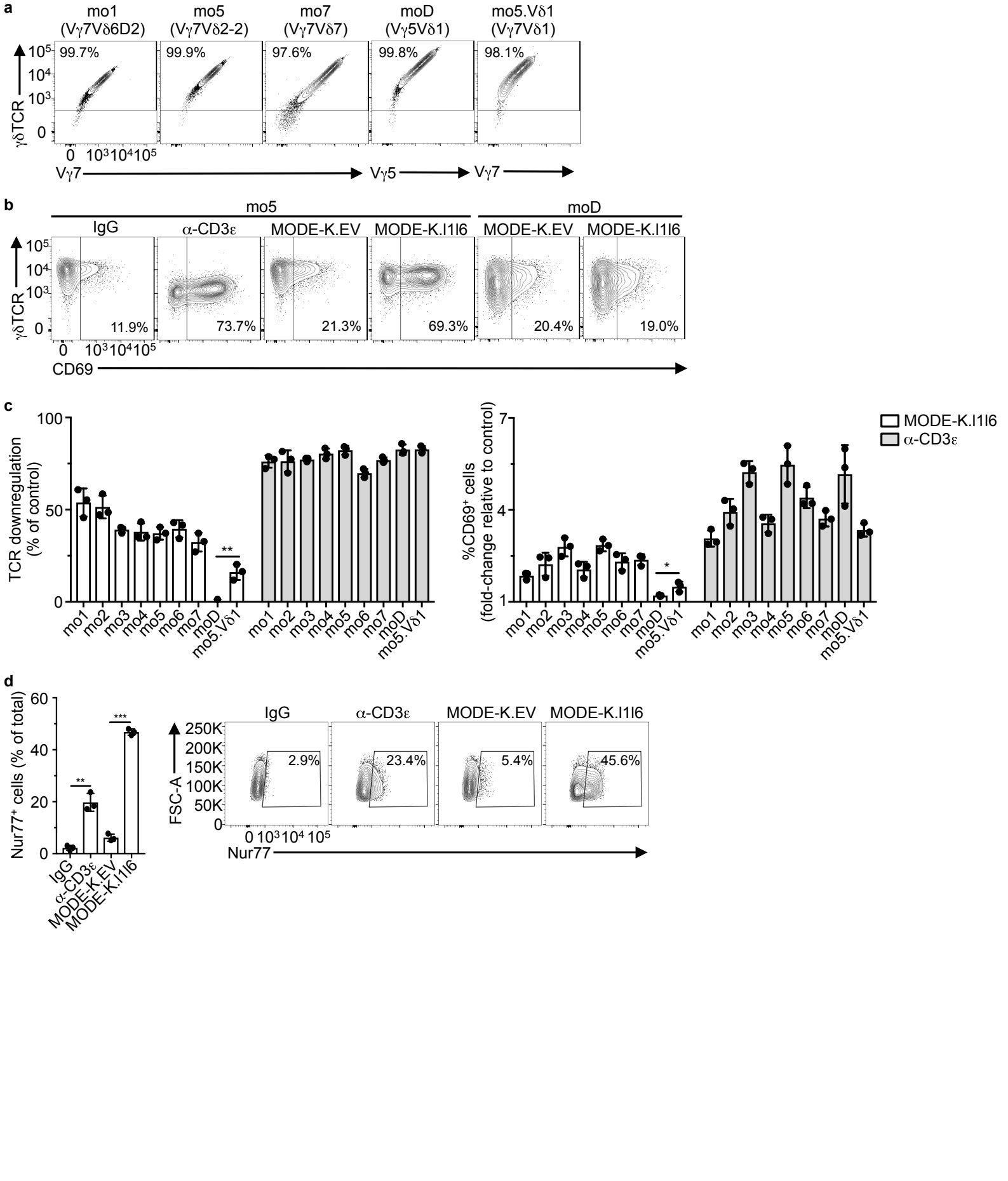
a
mo1 (Vγ7Vδ6D2)
mo5 (Vγ7Vδ2-2)
mo7 (Vγ7Vδ7)
moD (Vγ5Vδ1)
mo5.Vδ1 (Vγ7Vδ1)
99.7%
99.9%
97.6%
99.8%
98.1%
γδTCR
Vγ7
Vγ5
Vγ7
b
mo5
moD
IgG
α-CD3ε
MODE-K.EV
MODE-K.I1I6
MODE-K.EV
MODE-K.I1I6
11.9%
73.7%
21.3%
69.3%
20.4%
19.0%
γδTCR
CD69
c
TCR downregulation (% of control)
%CD69+ cells (fold-change relative to control)
MODE-K.I1I6
α-CD3ε
mo1
mo2
mo3
mo4
mo5
mo6
mo7
moD
mo5.Vδ1
d
Nur77+ cells (% of total)
IgG
α-CD3ε
MODE-K.EV
MODE-K.I1I6
FSC-A
Nur77
2.9%
23.4%
5.4%
45.6%

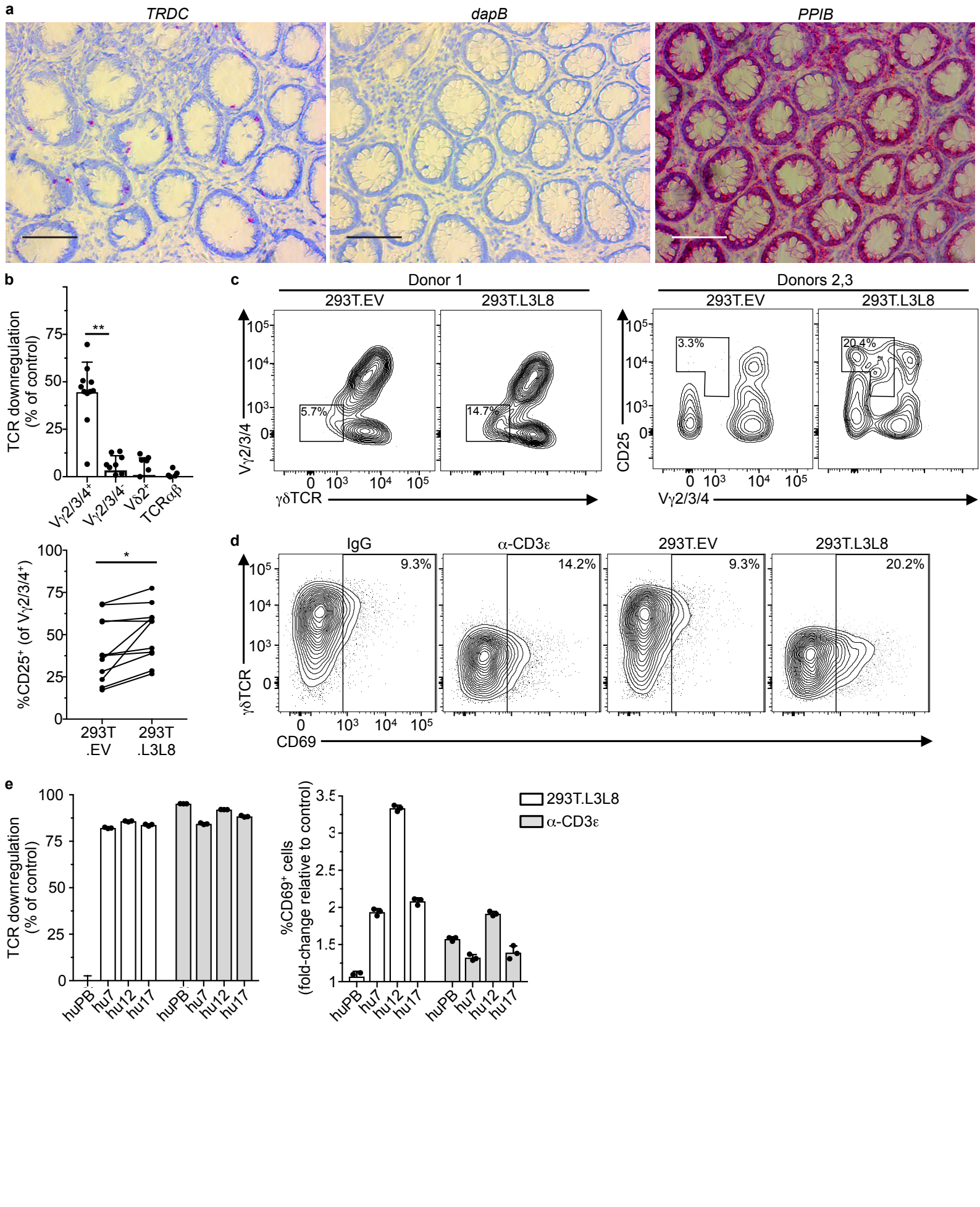
a
TRDC
dapB
PPIB
b
TCR downregulation (% of control)
**
Vγ2/3/4+
Vγ2/3/4-
Vδ2+
TCRαβ
%CD25+ (of Vγ2/3/4+)
*
293T .EV
293T .L3L8
c
Donor 1
293T.EV
293T.L3L8
5.7%
14.7%
Vγ2/3/4
γδTCR
Donors 2,3
3.3%
20.4%
CD25
d
IgG
α-CD3ε
9.3%
14.2%
20.2%
CD69
e
TCR downregulation (% of control)
huPB
hu7
hu12
hu17
%CD69+ cells (fold-change relative to control)
293T.L3L8
α-CD3ε

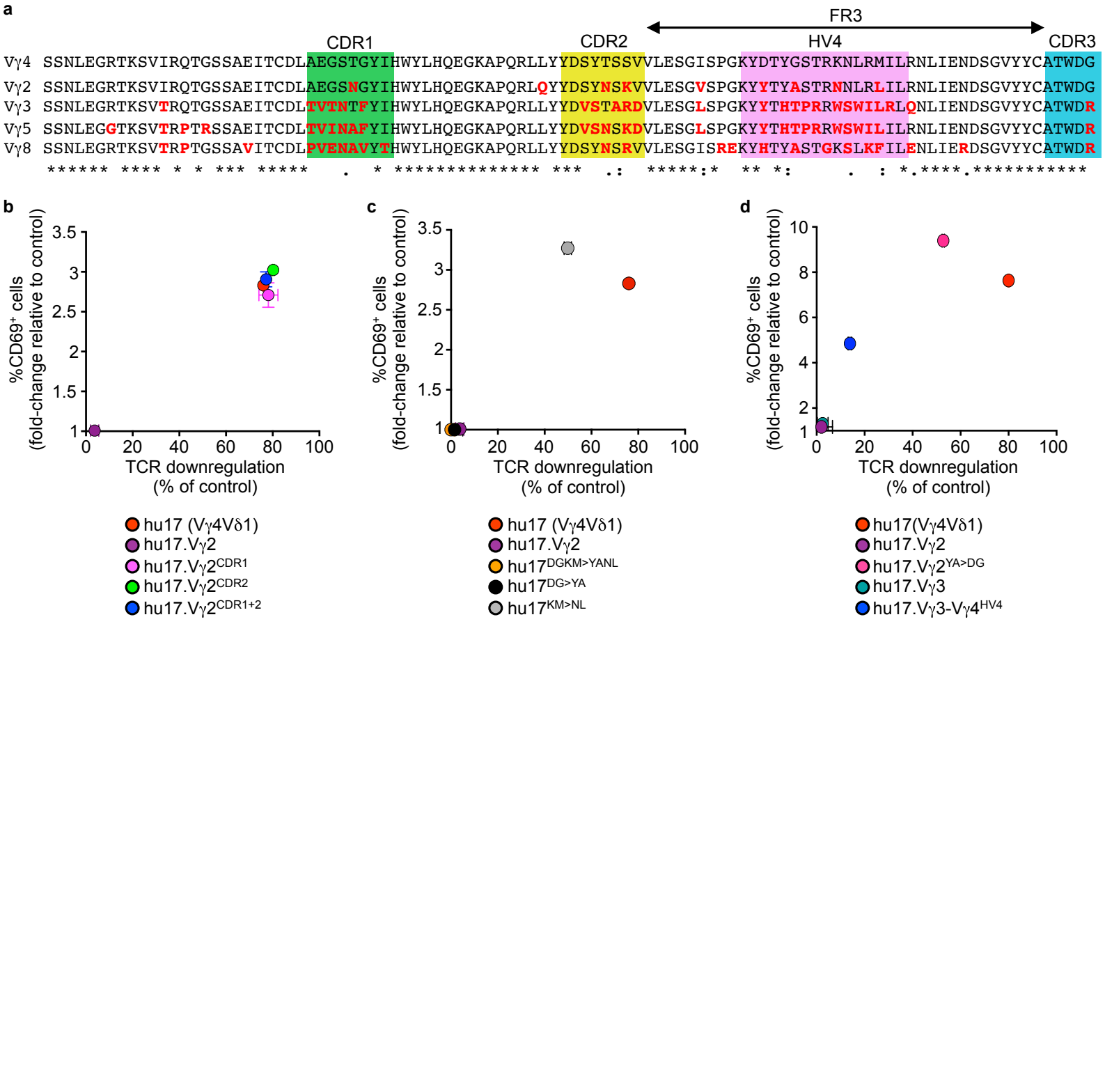
a
FR3
CDR1
CDR2
HV4
CDR3
Vγ4 SSNLEGRTKSVIRQTGSSAEITCDLAEGSTGYIHWYLHQEGKAPQRLLYYDSYTSSVVLESGISPGKYDTYGSTRKNLRMILRNLIENDSGVYYCATWDG
Vγ2 SSNLEGRTKSVIRQTGSSAEITCDLAEGSNGYIHWYLHQEGKAPQRLQYYDSYNSKVVLESGVSPGKYYTYASTRNNLRLILRNLIENDSGVYYCATWDG
Vγ3 SSNLEGRTKSVTRQTGSSAEITCDLTVTNTFYIHWYLHQEGKAPQRLLYYDVSTARDVLESGLSPGKYYTHTPRRWSWILRLQNLIENDSGVYYCATWDR
Vγ5 SSNLEGGTKSVTRPTRSSAEITCDLTVINAFYIHWYLHQEGKAPQRLLYYDVSNSKDVLESGLSPGKYYTHTPRRWSWILILRNLIENDSGVYYCATWDR
Vγ8 SSNLEGRTKSVTRPTGSSAVITCDLPVENAVYTHWYLHQEGKAPQRLLYYDSYNSRVVLESGISREKYHTYASTGKSLKFILENLIERDSGVYYCATWDR
b
%CD69+ cells (fold-change relative to control)
TCR downregulation (% of control)
hu17 (Vγ4Vδ1)
hu17.Vγ2
hu17.Vγ2CDR1
hu17.Vγ2CDR2
hu17.Vγ2CDR1+2
c
%CD69+ cells (fold-change relative to control)
TCR downregulation (% of control)
hu17 (Vγ4Vδ1)
hu17.Vγ2
hu17DGKM>YANL
hu17DG>YA
hu17KM>NL
d
%CD69+ cells (fold-change relative to control)
TCR downregulation (% of control)
hu17(Vγ4Vδ1)
hu17.Vγ2
hu17.Vγ2YA>DG
hu17.Vγ3
hu17.Vγ3-Vγ4HV4

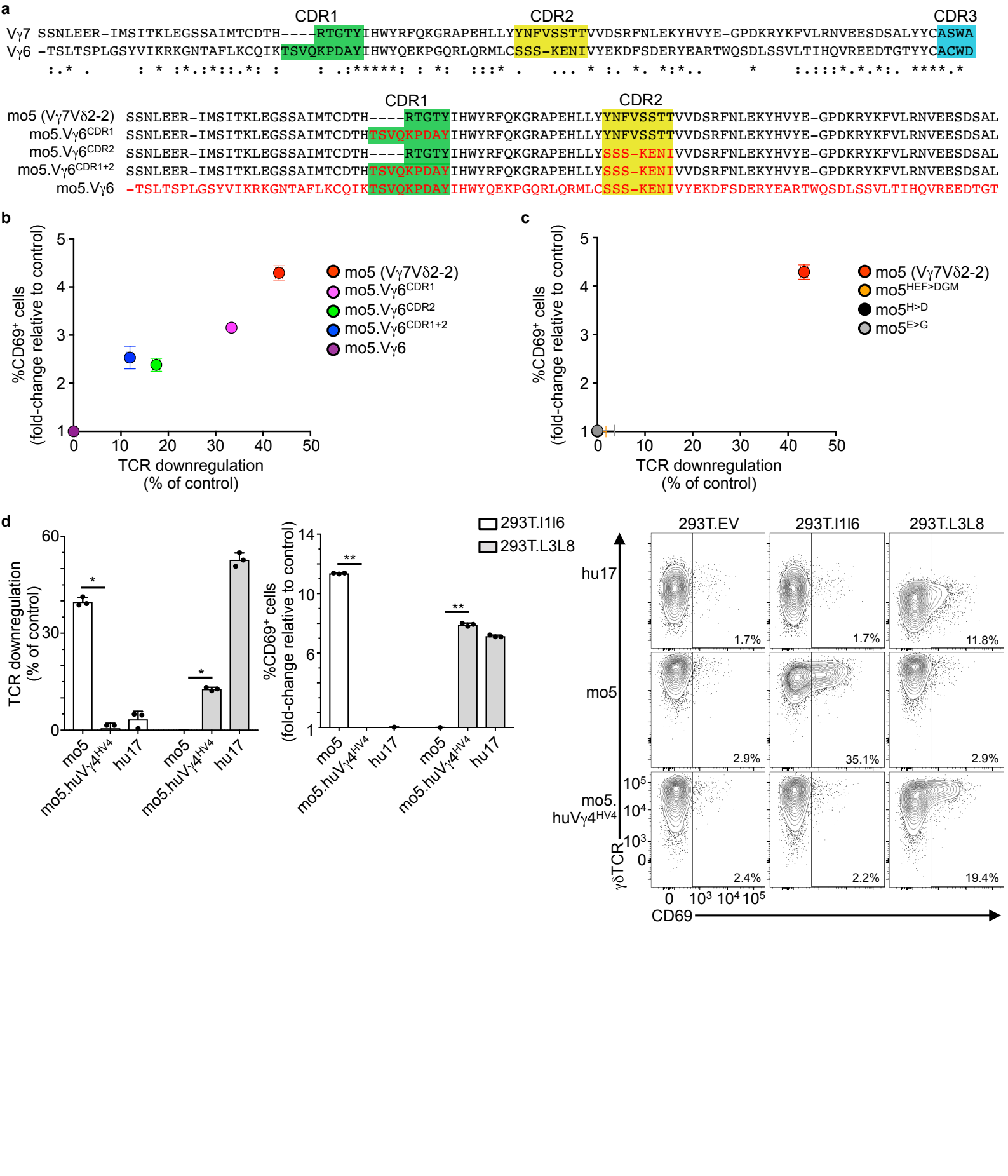
a
CDR1
CDR2
CDR3
Vγ7 SSNLEER-IMSITKLEGSSAIMTCDTH----RTGTYIHWYRFQKGRAPEHLLYYNFVSSTTVVDSRFNLEKYHVYE-GPDKRYKFVLRNVEESDSALYYCASWA
Vγ6 -TSLTSPLGSYVIKRKGNTAFLKCQIKTSVQKPDAYIHWYQEKPGQRLQRMLCSSS-KENIVYEKDFSDERYEARTWQSDLSSVLTIHQVREEDTGTYYCACWD
mo5 (Vγ7Vδ2-2) SSNLEER-IMSITKLEGSSAIMTCDTH----RTGTYIHWYRFQKGRAPEHLLYYNFVSSTTVVDSRFNLEKYHVYE-GPDKRYKFVLRNVEESDSAL
mo5.Vγ6CDR1 SSNLEER-IMSITKLEGSSAIMTCDTHTSVQKPDAYIHWYRFQKGRAPEHLLYYNFVSSTTVVDSRFNLEKYHVYE-GPDKRYKFVLRNVEESDSAL
mo5.Vγ6CDR2 SSNLEER-IMSITKLEGSSAIMTCDTH----RTGTYIHWYRFQKGRAPEHLLYSSS-KENIVVDSRFNLEKYHVYE-GPDKRYKFVLRNVEESDSAL
mo5.Vγ6CDR1+2 SSNLEER-IMSITKLEGSSAIMTCDTHTSVQKPDAYIHWYRFQKGRAPEHLLYSSS-KENIVVDSRFNLEKYHVYE-GPDKRYKFVLRNVEESDSAL
mo5.Vγ6 -TSLTSPLGSYVIKRKGNTAFLKCQIKTSVQKPDAYIHWYQEKPGQRLQRMLCSSS-KENIVYEKDFSDERYEARTWQSDLSSVLTIHQVREEDTGT
b
%CD69+ cells (fold-change relative to control)
TCR downregulation (% of control)
mo5 (Vγ7Vδ2-2)
mo5.Vγ6CDR1
mo5.Vγ6CDR2
mo5.Vγ6CDR1+2
mo5.Vγ6
c
%CD69+ cells (fold-change relative to control)
TCR downregulation (% of control)
mo5 (Vγ7Vδ2-2)
mo5HEF>DGM
mo5H>D
mo5E>G
d
TCR downregulation (% of control)
%CD69+ cells (fold-change relative to control)
293T.I1I6
293T.L3L8
mo5
mo5.huVγ4HV4
hu17
293T.EV
293T.I1I6
293T.L3L8
hu17
mo5
mo5. huVγ4HV4
γδTCR
CD69
1.7%
1.7%
11.8%
2.9%
35.1%
2.9%
2.4%
2.2%
19.4%

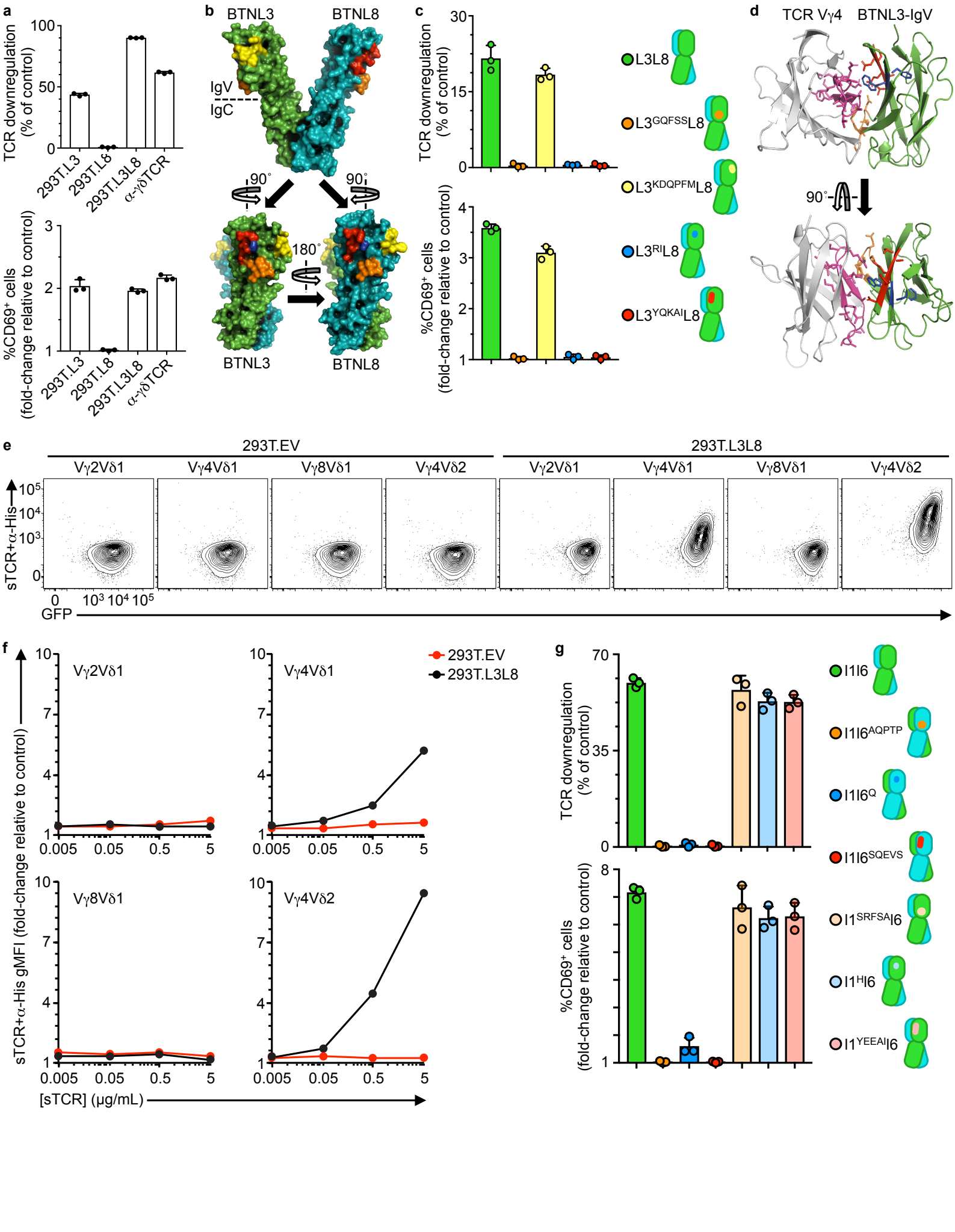
a
TCR downregulation (% of control)
293T.L3
293T.L6
293T.L3L8
α-γδTCR
%CD69⁺ cells (fold-change relative to control)
b
BTNL3
BTNL8
IgV
IgC
90˚
180˚
c
L3L8
L3GQFSSL8
L3KDQPFML8
L3RIL8
L3YQKAIL8
d
TCR Vγ4
BTNL3-IgV
e
293T.EV
293T.L3L8
Vγ2Vδ1
Vγ4Vδ1
Vγ8Vδ1
Vγ4Vδ2
sTCR+α-His
GFP
f
293T.EV
293T.L3L8
sTCR+α-His gMFI (fold-change relative to control)
[sTCR] (μg/mL)
g
I1I6
I1I6AQPTP
I1I6Q
I1I6SQEVS
I1SRFSAI6
I1HI6
I1YEEAII6

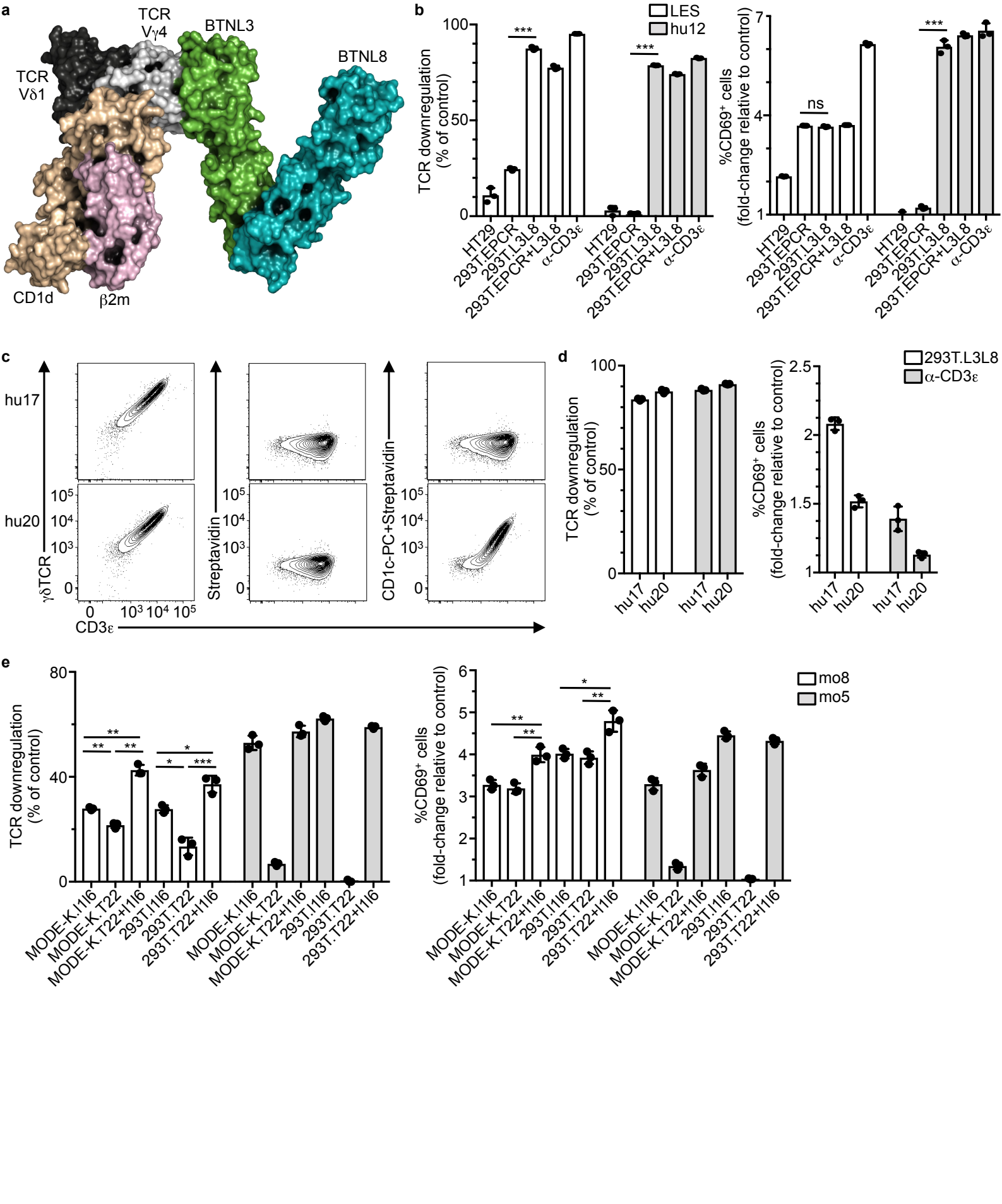
a
TCR Vγ4
BTNL3
BTNL8
TCR Vδ1
CD1d
β2m
b
LES
hu12
TCR downregulation (% of control)
%CD69⁺ cells (fold-change relative to control)
ns
***
HT29
293T.EPCR
293T.L3L8
293T.EPCR+L3L8
α-CD3ε
c
hu17
hu20
γδTCR
CD3ε
Streptavidin
CD1c-PC+Streptavidin
d
293T.L3L8
α-CD3ε
e
mo8
mo5
MODE-K.I1I6
MODE-K.T22
MODE-K.T22+I1I6
293T.I1I6
293T.T22
293T.T22+I1I6

TABLES

		CDR3γ			CDR3δ		
Clone	**V usage**	**AA sequence**	**Freq. average [indep. pools]**	**Ranks in indep. Pools**	**AA sequence**	**Freq. average [in indep pools]**	**Ranks in indep. Pools**
mo1	Vγ7Vδ6D2	ASWAYSSGFHKV	5.2% [5.5 / 5.7 / 4.3]	3 / 2 / 4	ALSEPWHIGGIRATDKLV	0.04% [0.03 / 0.09 / 0]	403 / 189 / n.f.
mo2	Vγ7Vδ6D2	ASWADSSGFHKV	2.8% [2.9 / 2.7 / 2.9]	7 / 8 / 9	ALSELSEGYEPATDKLV	0 [0 / 0 / 0]	n.f. / n.f. / n.f.
mo3	Vγ7Vδ2-2	ASWARYSSGFHKV	1.3% [1.2 / 1.2 / 1.4]	21 / 21 / 14	ALMGIGGLATDKLV	0.002% [0 / 0 / 0.006]	n.f. / n.f. / 1177
mo4	Vγ7Vδ2-2	ASWAGYSSGFHKV	20.3% [17.8 / 22.8 / 20.0]	1 / 1 / 1	ALMERGTEGYATDKLV	0.0007% [0 / 0.002 / 0]	n.f. / 3544 / n.f.
mo5	Vγ7Vδ2-2	ASWAGYSSGFHKV	20.2% [17.8 / 22.8 / 20.0]	1 / 1 / 1	ALMERGRRDTSLTDKLV	0.013% [0 / 0.04 / 0]	n.f. / 279 / n.f.
mo6	Vγ7Vδ7	ASWALSSGFHKV	0.03% [0.007 / n.f. / 0.08]	366 / n.f. / 108	AMGYRRDTDKLV	0.75% [1.5 / 0.002 / 0.8]	8 / 2066 / 25
mo7	Vγ7Vδ7	ASWGYSSGFHKV	5.4% [5.8 / 4.5 / 5.8]	2 / 3 / 2	AMGATDKLV	0.2% [0 / 0.6 / 0]	n.f. / 16 / n.f.

Table 1. Murine γδTCR chain pairs used for T cell transduction.

Amino acid sequences (non-germline in red) of the CDR3γ and δ pairs cloned into lentiviral vector (LV) backbones. Corresponding frequencies (freq.) and ranks for each sequence in the deep-sequencing data (see Fig. 1) are indicated (n.f., not found).

			CDR3γ			CDR3δ		
Donor	**Clone**	**V usage**	**AA sequence**	**Freq.**	**Rank**	**AA sequence**	**Freq.**	**Rank**
1	hu1	Vγ4Vδ1	ATWDPGWFKI	0	n.f	ALGEIGYWGIHRVNKLI	0	n.f
	hu2	Vγ4Vδ3	ATWDWGYYKKL	0	n.f	ASGDTTDKLI	0	n.f
	hu3	Vγ4Vδ3	ATWAGYYKKL	n.f	n.f	AAMGVPFLEGDTGPKLI	0	n.f
	hu4	Vγ2Vδ1	ATWKSSDWIKT	n.f	n.f	ALGELGYPDKLI	0.02%	1118
2	hu5	Vγ4Vδ1	ATWDGACTTGWFKI	n.f	n.f	ALGEKMGPNKLI	0	n.f
	hu6	Vγ4Vδ1	ATWDGACTTGWFKI	n.f	n.f	ALGPYRVRLIDKLI	0	n.f
	hu7	**Vγ4Vδ1**	**ATWDGPWNYYKKL**	**0.13%**	**88**	**ALGERGYWGILGDKLI**	**0**	**n.f**
	hu8	Vγ4Vδ3	ATWAPYYKKL	0.21%	49	AFCSVYWGICTDKLI	3.3%	6
	hu9	Vγ4Vδ3	ATWDGPNYKKL	11%	2	AFFFGWGIRFYTDKLI	42.7%	1
3	hu10	Vγ4Vδ3	ATWETYYKKL	3.4%	4	AFMFPPVGGLLI	36.6%	1
	hu11	Vγ4Vδ1	AIANYYKKL	0.04%	216	ALGELLYVGGIIDKLI	0	n.f
	hu12	**Vγ4Vδ1**	**ATWVMAHYKKL**	**3.6%**	**3**	**ALGERESLYKLI**	**7.5%**	**2**
	hu13	Vγ4Vδ1	ATWDGPVL	0.8%	17	ALGESTGPYWGIRGYTDKLI	2.0%	13
	hu14	Vγ4Vδ1	ATWVPGWFKI	0.44%	36	ALGELREWGTGVYTDKLI	1.2%	18
	hu15	Vγ4Vδ1	ATWDGRGATGWFKI	0.63%	28	ALGCQYWGIQADKLI	2.2%	12
	hu16	Vγ2Vδ3	ATWDGPHYKKL	10.4%	2	AFMFPPVGGLLI	36.6%	1
	hu17	**Vγ4Vδ1**	**ATWDGSKKL**	**0.2%**	**72**	**ALGESSLGYWGILADKLI**	**0**	**n.f**
	hu18	Vγ4Vδ1	ATWDAFGWFKI	0	n.f	ALGELELRLKIPGTDKLI	3.9%	6
	hu19	Vγ4Vδ3	ATWDCRYKKL	0	n.f	AFLPYWGIRKGSDTLTDKLI	0	n.f
4	hu20	Vγ4Vδ1	ATWDGYKKL	N/A	N/A	ALGPPLFYVLGYRKLI	N/A	N/A
5	huPB	Vγ9Vδ2	ALWEKQQELGKKIK V	N/A	N/A	ACDPLGNQYTDKLI	N/A	N/A
6	sk1	Vγ4Vδ1	ATWELNYYKKL	N/A	N/A	ALGTIRPSPFLLGGYLTRTTDKLI	N/A	N/A
	sk2	Vγ4Vδ1	ATWDGYYKKL	N/A	N/A	ALGEKITFLGNGWGRHTDKLI	N/A	N/A

Table 2. Human γδTCR chain pairs used for T cell transduction.

Amino acid sequences (non-germline in red) of the CDR3γ and δ sequenced from colonic IELs responding to BTNL3+8 (donors 1-3, hu1-19; see Fig. 3), with corresponding frequencies (freq.) and ranks in the corresponding deep-sequencing data (n.f, not found); from colonic IELs stained by CD1c-PC dextramers (donor 4, hu20; see Fig. 7); from peripheral blood γδ lymphocytes (donor 5, huPB), and from skin-derived IEL (donor 6, sk1-2; see Supplementary Fig. 7c). Lymphocytes isolated from donors 4-6 were not subjected to deep sequencing (N/A, not applicable).

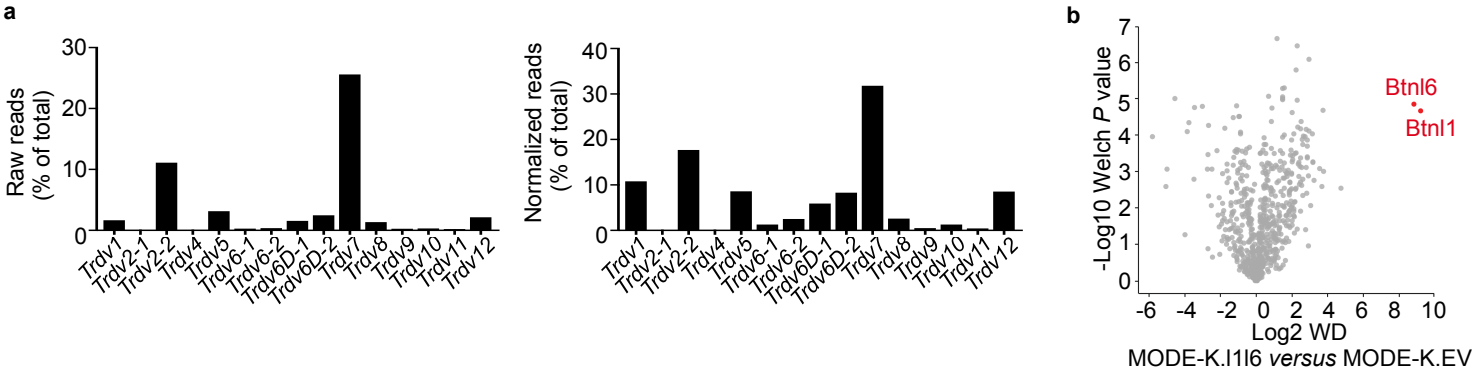

Supplementary Fig. 1. Delta chain usage of Vγ7⁻ IEL, and Btnl1+6 co-precipitation

a, TCR analysis of *Trdv* gene usage by Vγ7⁻ IEL sorted in parallel to the Vγ7⁺ IEL from Fig. 1a,b,c. Data derived from cells sorted from pooled mice IEL (n = 8). Representative of three independent sorts. **b**, Volcano plot representation of a mass-spectrometry analysis following anti-Flag pull-down on lysates from MODE-K.EV or MODE-K.l1l6 cells. Data expressed as the mean Welch difference in protein intensities in MODE-K.l1l6 *versus* MODE-K.EV samples (x-axis; Welch difference, WD) and associated *P* values (y-axis) for each protein (represented by dots), from multiple mass-spectrometry analysis replicates (n = 3)

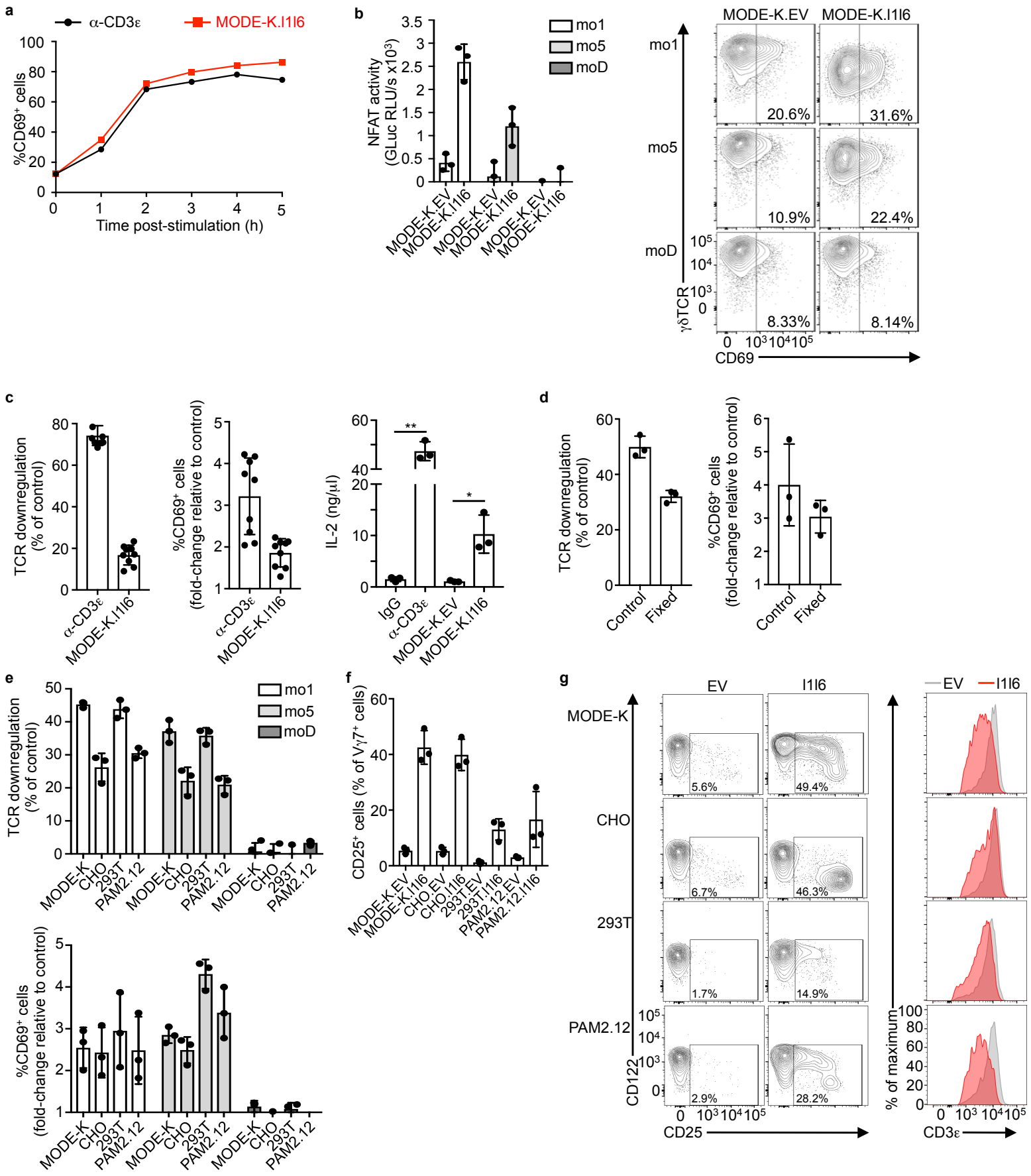

Supplementary Fig. 2. Requirements for a Btnl1+6-dependent response.

a, Flow cytometry analysis of the proportion of CD69⁺ J76-mo5 cells (y-axis) co-cultured with α-CD3ε or MODE-K.I1I6 over time (x-axis). Data expressed as mean of two experiments. **b,** Quantification of NFAT promoter activity (left) in JRT3.NFAT-GLuc cells transduced with the indicated TCRs and co-cultured with MODE-K.EV or MODE-K.I1I6 cells for 24 h. Gaussia Luciferase (GLuc) was measured in supernatants (RLU/s, relative light units per second). Data expressed as mean±s.d. (n = 3) and representative of two experiments. Cells were analysed in parallel by flow cytometry for γδTCR and CD69 expression (right) as a positive control of the response to MODE-K.I1I6 cells. **c**, Flow cytometry analysis of TCR downregulation (left), CD69 upregulation (centre) and ELISA quantification of IL-2 production (right) by E6.1-mo5 cells co-cultured with the indicated antibodies or cells lines. Flow cytometry data acquired after 5 h, expressed as mean±s.d., normalized to IgG or MODE-K.EV; pooled from nine independent experiments. ELISA data acquired after 24 h, expressed as mean±s.d. (n = 3); representative of three experiments. **d**, Flow cytometry analysis of TCR downregulation (left) and CD69 upregulation (right) by J76-mo5 cells co-cultured with untouched (control) or fixed MODE-K.I1I6 cells for 5 h. Data expressed as mean±s.d., normalized to MODE-K.EV; pooled from three independent experiments. **e**, Flow cytometry analysis of TCR downregulation (top) and CD69 upregulation (bottom) by J76-mo1, -mo5 or -moD cells co-cultured the indicated cell lines transduced with Btnl1+6. Data expressed as mean±s.d., normalized to corresponding cell line transduced with empty vector; pooled from three independent experiments. **f**, Flow cytometry analysis of the proportion of CD25⁺ cells in Vγ7⁺ IEL co-cultured with the indicated cell lines overnight. Data from individual mice expressed as mean±s.d. (n = 3). **g**, Flow cytometry analysis of CD25, CD122 and CD3ε expression by Vγ7⁺ IEL co-cultured with the indicated cell lines transduced with EV or Btnl1+6 (I1I6) overnight. Representative of co-cultures from individual mice (n = 3), related to (f).

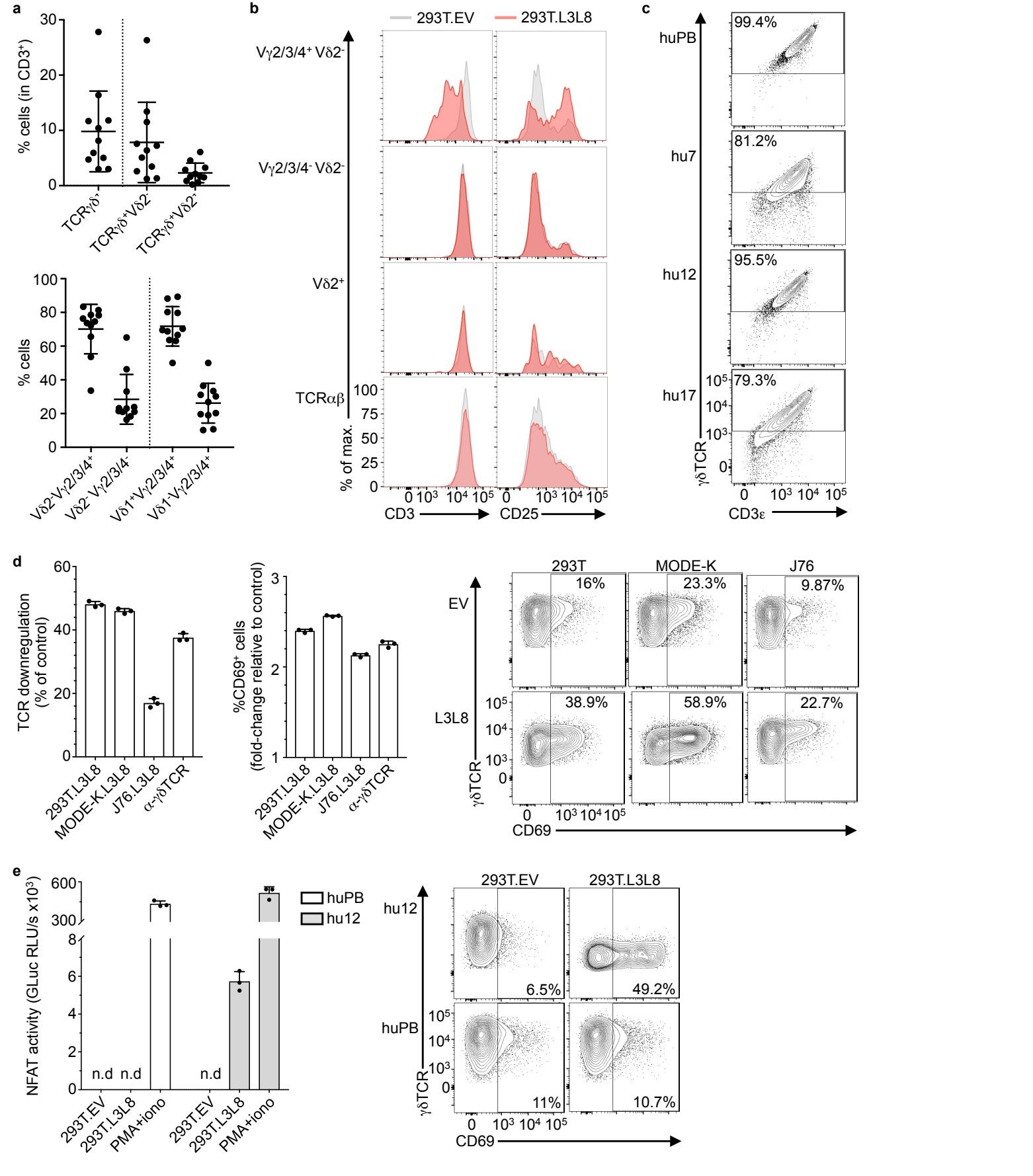

Supplementary Figure 3. The transfer of Vγ4⁺ TCRs from responding IELs confers reactivity to BTNL3+8.

a, Flow cytometry analysis of colonic γδ T cell composition, as proportion of total CD3⁺ cells (top); Vγ2/3/4 chain usage of TCRγδ⁺Vδ2⁻ cells and Vδ chain usage of Vδ2⁻Vγ2/3/4⁺ cells (bottom), after a 5 days culture. Data expressed as mean±s.d. of independent patient biopsies (n = 11). **b,** Flow cytometry analysis of CD3 and CD25 expression by the indicated human colonic lymphocyte subsets after co-culture with 293T.EV (grey) or .L3L8 (red) overnight. Representative of independent patient samples (n = 11). **c,** Flow cytometry analysis of CD3ε and γδTCR expression by J76 cells transduced with the indicated TCRs, 96h post-transduction. Representative of three independent experiments. **d,** Flow cytometry analysis of TCR downregulation (left) and CD69 upregulation (centre) by J76-hu12 cells co-cultured with the indicated cells lines or α-γδTCR antibody for 5 h. Data expressed as mean±s.d (n = 3), normalized to the matching cell lines transduced with empty vector, or control IgG. Corresponding raw flow cytometry plots are shown on the right. Representative of two (J76) or three (MODE-K) independent experiments (293T). **e,** Quantification of NFAT promoter activity (left) in JRT3.NFAT-GLuc cells transduced with the indicated TCRs and co-cultured with 293T.EV or 293T.L3L8 cells, or stimulated with PMA and ionomycin (PMA+iono) for 24 h. Gaussia luciferase (GLuc) was measured in supernatants (RLU/s, relative light units per second). Data expressed as mean±s.d (n = 3); n.d, non-detectable above background. Cells were analysed in parallel by flow cytometry for γδTCR and CD69 expression (right) as a positive control of the response to 293T.L3L8 cells. Representative of two independent experiments.

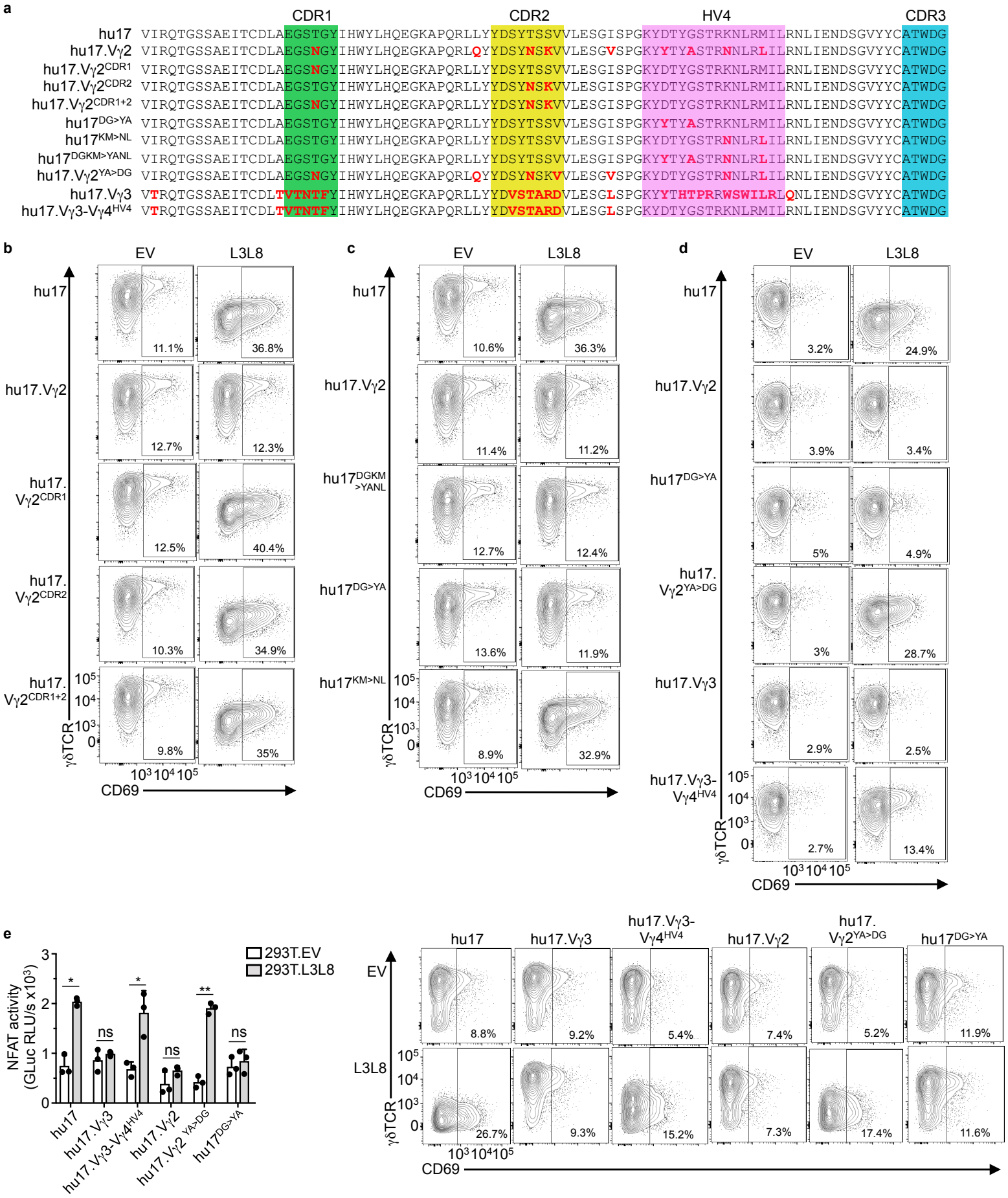

Supplementary Fig. 4. hu17 TCR variants and their responses to L3L8

a, Alignment of hu17 variants tested in Fig. 4b,c,d. Differences from the wild-type Vγ4 sequence are in bold red. CDR1/2/3 and HV4 are highlighted in green, yellow, cyan and pink, respectively. **b,c,d,** Flow cytometry analysis of γδTCR and CD69 expression by J76 cells transduced with the indicated hu17 TCR variants and co-cultured with 293T.EV or 293T.L3L8 cells for 5 h. Representative of individual co-cultures (n = 3), related to Fig. 4b,c,d. **e,** Quantification of NFAT promoter activity (left) in JRT3.NFAT-GLuc cells transduced with the indicated hu17 TCR variants and co-cultured with 293T.EV or 293T.L3L8 cells for 24 h. GLuc was measured in supernatants (RLU/s, relative light units per second). Data expressed as mean±s.d. of individual co-cultures (n = 3). *P < 0.05; **P < 0.01; ns, not significant. Cells were analysed in parallel by flow cytometry for γδTCR and CD69 expression (right) as a positive control of the response to 293T.L3L8 cells.

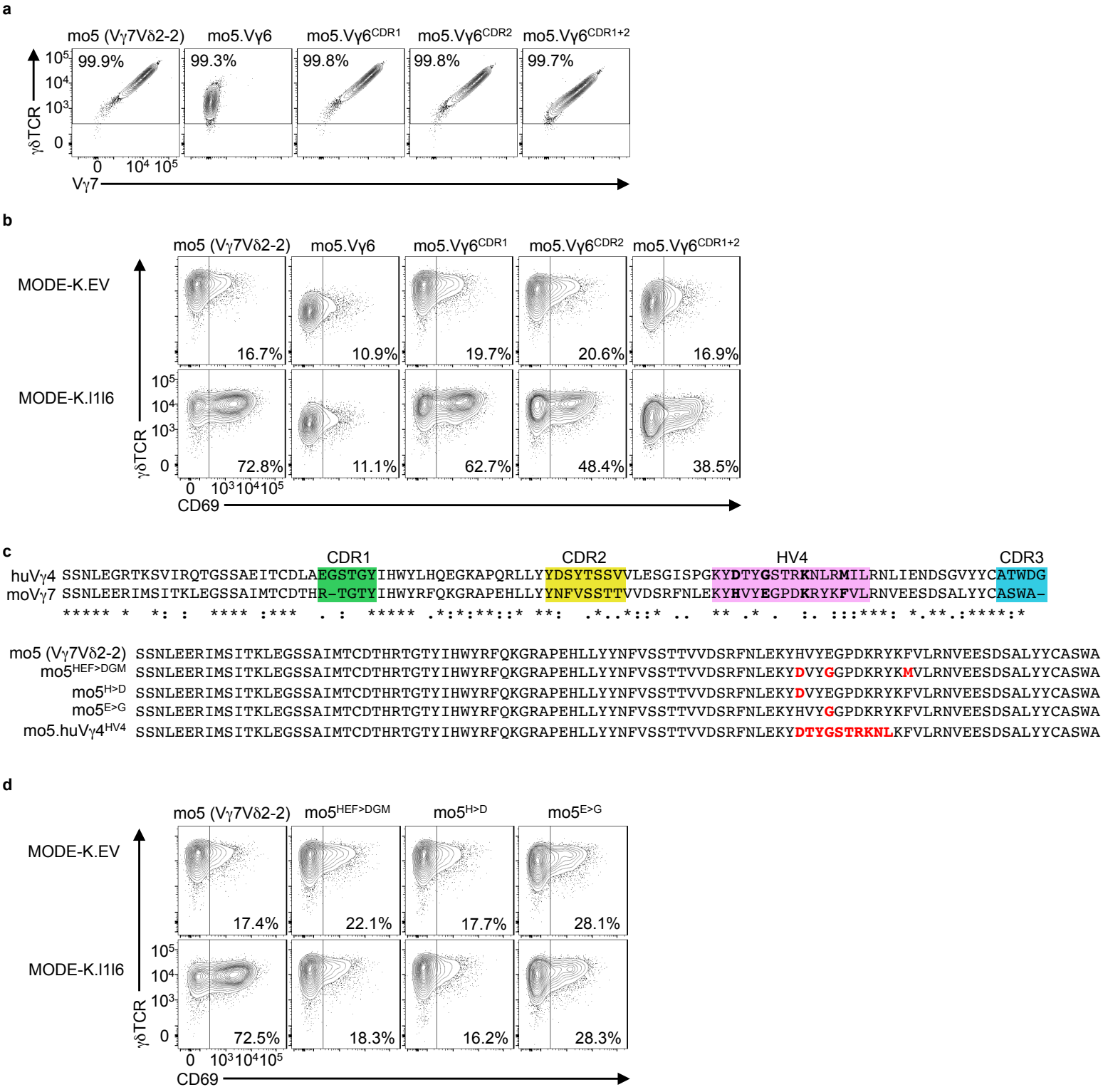

Supplementary Fig. 5. HV4 is required for responses to human and murine BTNL/Btnl

a, Flow cytometry analysis of Vγ7 and γδTCR expression by J76 cells transduced with the indicated TCRs and sorted to ensure equivalent expression. Representative of three independent experiments. **b,** Flow cytometry analysis of γδTCR and CD69 expression by J76 cells transduced with the indicated TCRs and co-cultured with MODE-K.EV or MODE-Kl1l6 cells for 5 h. Representative of individual co-cultures (n = 3), related to Fig. 5b. **c,** Alignments of mouse Vγ7 with human Vγ4 sequences (top; amino acids identified in Fig. 4c are bolded); and of mo5 variants tested in Fig. 5c,d (bottom; differences from wild-type Vγ7 sequence in bold red). **d,** Flow cytometry analysis of γδTCR and CD69 expression by J76 cells transduced with the indicated mo5 variants and co-cultured with MODE-K.EV or MODE-K.l1l6 cells for 5 h. Representative of individual co-cultures (n = 3), related to Fig. 5c.

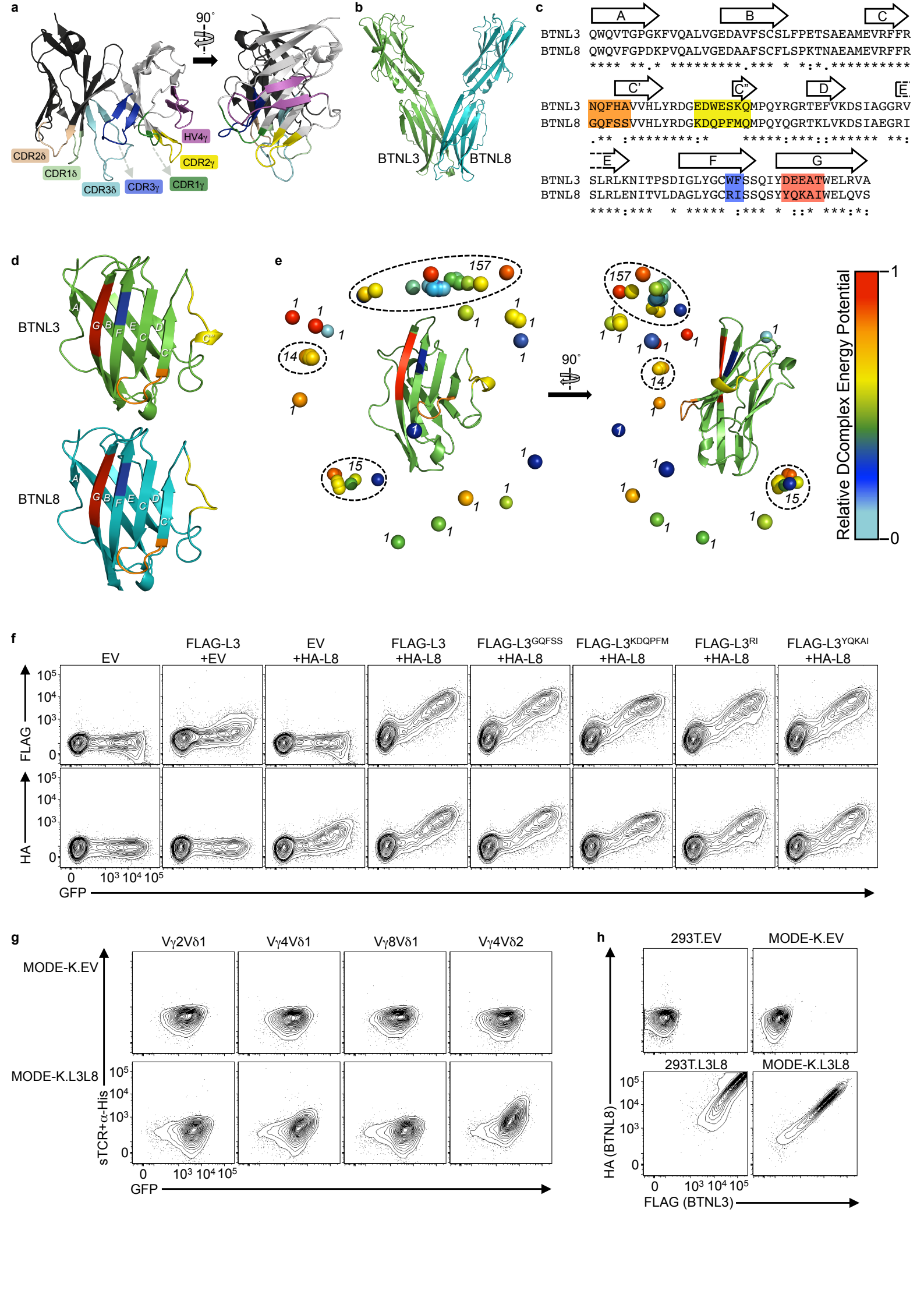
a
90˚
CDR2δ
CDR1δ
CDR3δ
CDR3γ
CDR1γ
HV4γ
CDR2γ
b
BTNL3
BTNL8
c
A
B
C
C'
C"
D
E
F
G
BTNL3 QWQVTGPGKFVQALVGEDAVFSCSLFPETSAEAMEVRFFR
BTNL8 QWQVFGPDKPVQALVGEDAAFSCFLSPKTNAEAMEVRFFR
BTNL3 NQFHAVVHLYRDGEDWESKQMPQYRGRTEFVKDSIAGGRV
BTNL8 GQFSSVVHLYRDGKDQPFMQMPQYQGRTKLVKDSIAEGRI
BTNL3 SLRLKNITPSDIGLYGCWFSSQIYDEEATWELRVA
BTNL8 SLRLENITVLDAGLYGCRISSQSYYQKAIWELQVS
d
BTNL3
BTNL8
e
90˚
Relative DComplex Energy Potential
1
0
f
EV
FLAG-L3 +EV
EV +HA-L8
FLAG-L3 +HA-L8
FLAG-L3GQFSS +HA-L8
FLAG-L3KDQPFM +HA-L8
FLAG-L3RI +HA-L8
FLAG-L3YQKAI +HA-L8
FLAG
HA
GFP
g
Vγ2Vδ1
Vγ4Vδ1
Vγ8Vδ1
Vγ4Vδ2
MODE-K.EV
MODE-K.L3L8
sTCR+α-His
GFP
h
293T.EV
MODE-K.EV
293T.L3L8
MODE-K.L3L8
HA (BTNL8)
FLAG (BTNL3)

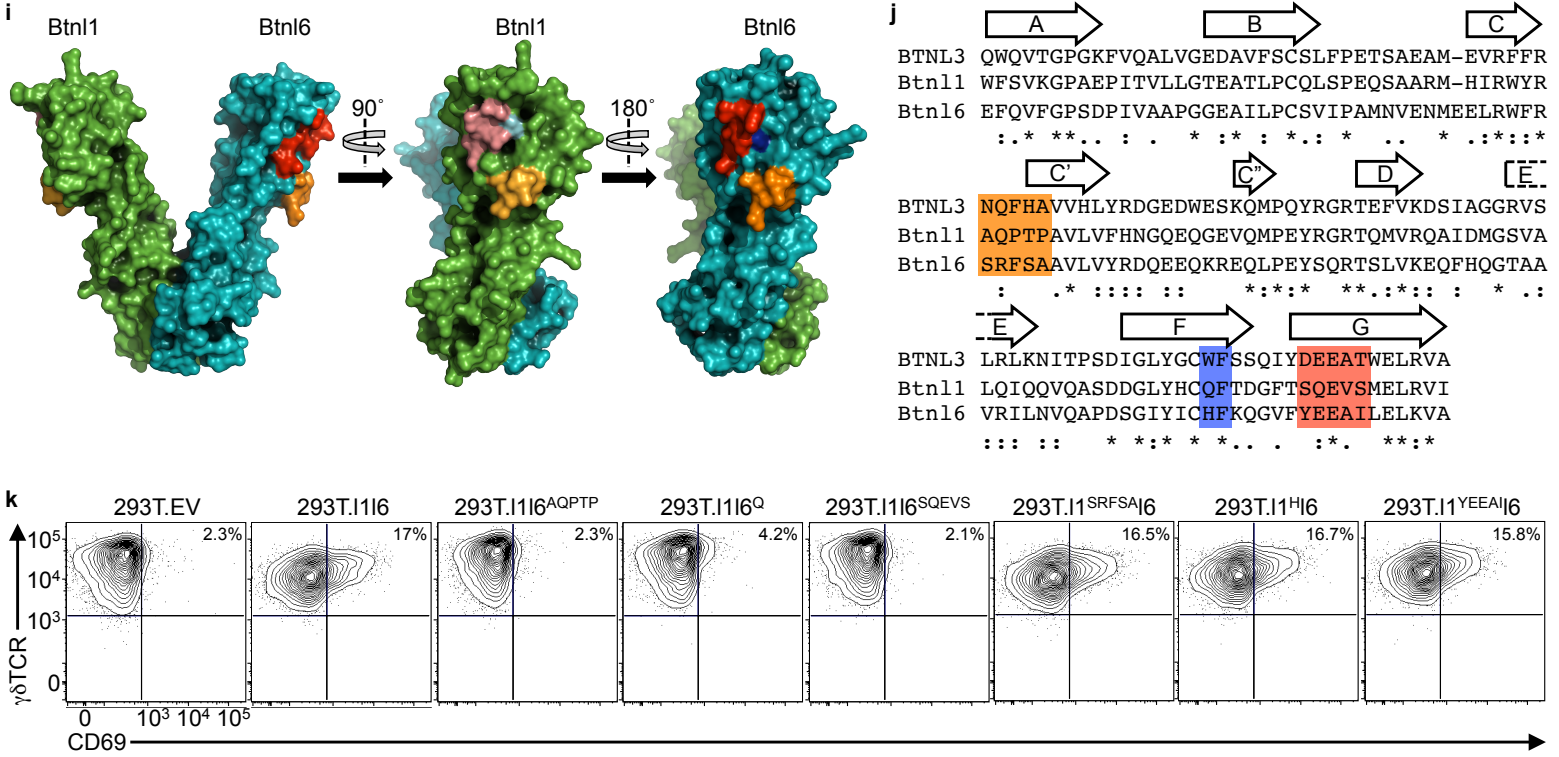

Supplementary Figure 6. Stepwise determination of the Vγ4 / BTNL3 interaction model

a, Cartoon representation of the crystal structure of a Vγ4Vδ1 TCR V-domains (from PDB 4MNG), with all CDRs and HV4γ highlighted. **b**, Cartoon representation of a BTNL3 (green) / BTNL8 (teal) heterodimer model, derived with 3D-JIGSAW from a BTN3A1 homodimer (PDB 4F80). **c**, Alignment of the IgV-domain sequences of BTNL3 and BTNL8. Canonical Ig-fold β-strands [A,B,C,C',C",D,E,F,G] are indicated with arrows. Solvent-exposed residues that are significantly different are highlighted in orange [NQFHA/GQFSS], yellow [EDWESK/KDQPFM], blue [WF/RI], and red [DEEAT/YQKAI]. **d**, Cartoon representation of the IgV-domains of BTNL3 (green) and BTNL8 (teal) from (b), with the same annotation as in (c). **e**, Cartoon representation of the results of 200 unrestricted docking simulation runs in SwarmDock, between the IgV-domain of BTNL3 (green) and the TCR Vγ4Vδ1 V-domains (PDB 4MNG). Each sphere represents the centroid of the TCR (numbers in italic indicate the number of solutions for groups) and are color-coded according to the relative energy between the docked poses (relative Docking Complex [DComplex] Energy Potential scale displayed on the right). Note that the IgV-domain of BTNL3 is rotated 45˚ counter-clockwise along the x-axis compared to (d). **f**, Flow cytometry analysis of FLAG-tagged BTNL3 and HA-tagged BTNL8 expression in 293T cells, 48 h post-transfection. Representative of three independent experiments. Related to Fig. 6c. **g**, Flow cytometry analysis of the binding of the indicated soluble TCRs (sTCR; pre-incubated with anti-6xHis tag antibody, α-His) after incubation with MODE-K.EV or MODE-K.L3L8 cells at 4˚C for 1 h. Representative of three independent experiments. Related to Fig. 6e. **h**, Flow cytometry analysis of FLAG-BTNL3 and HA-BTNL8 expression on the indicated cell lines that were used for the sTCR staining experiments. Related to (g) and Fig. 6e. **i**, Surface representation of a heterodimeric Btnl1 (green) / Btnl6 (teal) model, derived with 3D-JIGSAW from a BTN3A1 homodimer (PDB 4F80). Candidate CFG face motifs corresponding to the ones identified in BTNL3 (see Fig. 6b,c; and below) are highlighted in orange (AQPTP/SRFSA), blue (QF/HF), and red (SQEVS/YEEAI). **j**, Alignment of the IgV-domain sequences of BTNL3, Btnl1 and Btnl6. Canonical Ig-fold β-strands [A,B,C,C',C",D,E,F,G] are indicated with arrows. Candidates motifs are highlighted using the same colour-coding as in (i). **k**, Flow cytometry analysis of γδTCR and CD69 expression by J76-mo5 cells co-cultured with 293T cells expressed the indicated constructs for 5h. Representative of three independent experiments. Related to Fig. 6g.

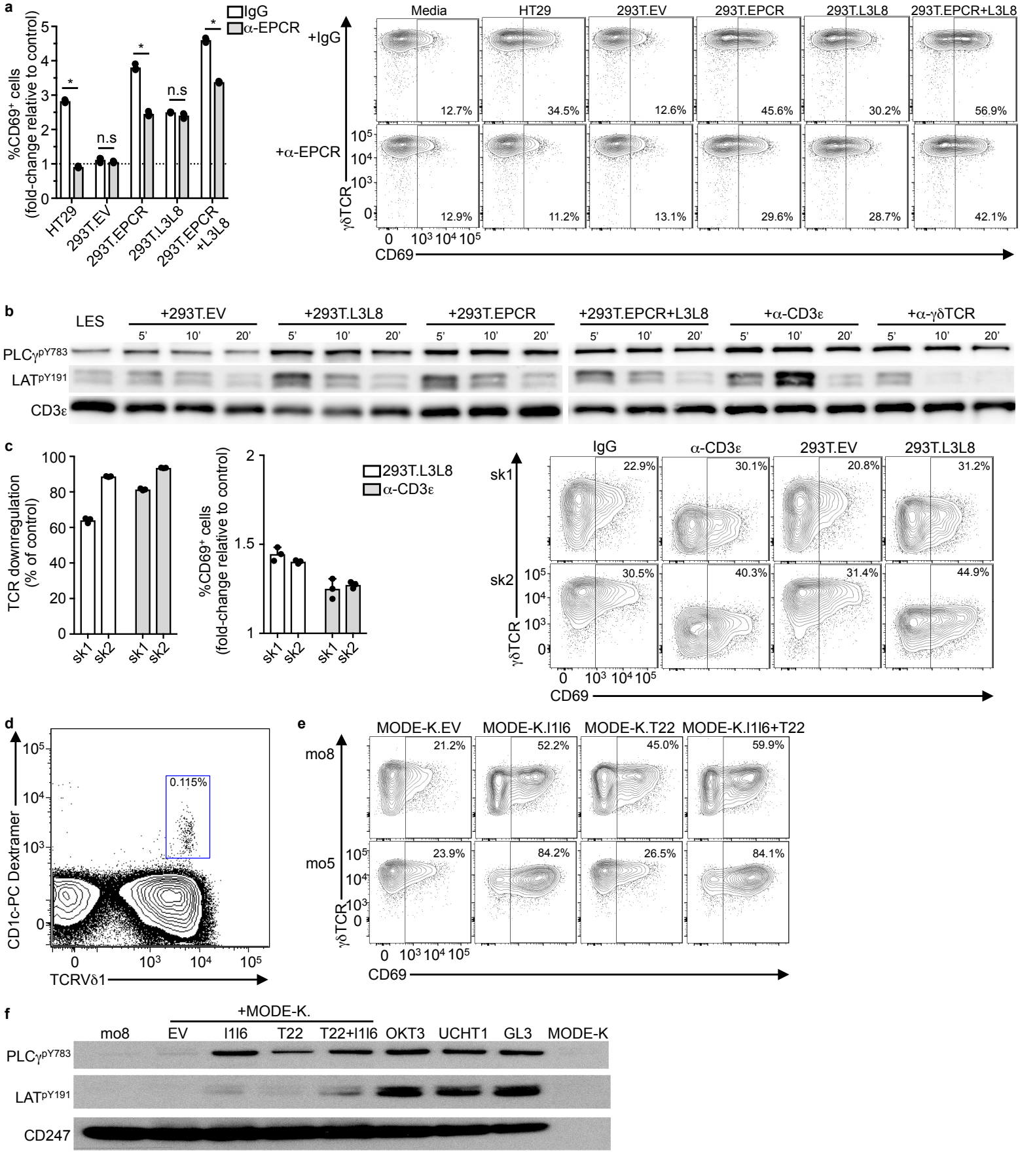

Supplementary Figure 7. Dual reactivity of human and mouse γδTCRs

a, Flow cytometry analysis of CD69 upregulation (left) by JRT3-LES cells co-cultured with the indicated cell in the presence of control IgG or α-EPCR antibodies (10 μg/mL) for 3 h. Data expressed as mean±s.d. of the proportion of CD69⁺ cells in individual co-cultures (n = 3). Corresponding raw flow cytometry plots are shown (right). Representative of two independent experiments. *P < 0.001; n.s, not significant. **b,** Western blot analysis of PLCγ and LAT phosphorylation in JRT3-LES cells co-cultured with the indicated cell lines or antibodies at 37˚C for the indicated times. CD3ε, loading control. Representative of three independent experiments. **c,** Flow cytometry analysis of TCR downregulation (left) and CD69 upregulation (centre) by J76 cells transduced with the indicated TCRs and co-cultured with 293T.L3L8 cells or α-CD3ε. Data expressed as mean±s.d. of individual co-cultures (n = 3), normalized to 293T.EV or control IgG. Corresponding examples of raw flow cytometry plots are shown (right). Representative of three independent experiments. **d,** Flow cytometry analysis of CD1c-PC dextramer binding to human colonic γδTCR⁺ cells. The gate used for single-cell sorting is shown. **e,** Flow cytometry analysis of γδTCR and CD69 expression by J76-mo8 and J76-mo5 cells after co-culture with the indicated cell lines. Representative of three individual co-cultures, related to Fig. 7e. **e,** Western blot analysis of PLCγ and LAT phosphorylation in J76-mo8 cells co-cultured with the indicated cell lines or antibodies at 37˚C for 10 min. CD247, loading control. Representative of three (PLCγ) and two (LAT) independent experiments.

V usage	Clone #	CDR3γ	CDR3δ
Vγ7Vδ7	1	ASWRYSSGFHKV	AMLATDKLV
	2 (mo7)	**ASWGYSSGFHKV**	**AMGATDKLV**
	3	ASWGYSSGFHKV	AIYRFTDKLV
	4	ASWGRYSSGFHKV	AIYRSTDKLV
	5	ASWAQYSSGFHKV	AVGWGDKLV
	6	ASWAYSSGFHKV	AMGRDNAKLV
	7	ASWVYSSGFHKV	APSTTATDKLV
	8	**ASWGYSSGFHKV**	**AWGIRATDKLV**
	9	**ASWAGLSSGFHKV**	**AWGIRATDKLV**
	10	**ASWAEYSSGFHKV**	**AWGIRATDKLV**
	11	ASWAGYSSGFHKV	AMPRDATDKLV
	12	ASWAGYSSGFHKV	AMGRGTTDKLV
	13	ASWAPYSSGFHKV	ARISEGYDDKLV
	14	ASWEYSSGFHKV	AYRRDTSTDKLV
	15	ASWAEGGYSSGFHKV	ACLYRRDTDKLV
	16	ASWALYSSGFHKV	AMVGGIRVDKLV
	17 (mo6)	**ASWALSSGFHKV**	**AMGYRRDTDKLV**
	18	ASWAYSSGFHKV	AMLPRDTSSDKLV
	19	ASWGYSSGFHKV	ATYRRDTGTDKLV
	20	ASWAHSSGFHKV	AMVPYRRDTDKLV
	21	ASWAGRGSSGFHKV	AMVDIGGINTDKLV
	22	**ASWAYSSGFHKV**	**AMERISEGYELGKLV**
	23	ASWAEYSSGFHKV	AMEQVAGGIRTDKLV
	24 (mo8)	ASWAGYSSGFHKV	AMERWEGYELTDKLV
	25	ASWEYSSGFHKV	AMAIYRRDTRATDKLV
Vγ7Vδ2-2	26	ASWAGGGSSGFHKV	ALLEGPLSSDKLV
	27	ASWTYSSGFHKV	ALMASEGYADKLV
	28	ASWAGYSSGFHKV	ALMERGRGIADKLV
	29 (mo3)	**ASWARYSSGFHKV**	**ALMGIGGLATDKLV**
	30	ASWAGGGSGFHKV	ALMERGEGYEITDKLV
	31 (mo4)	**ASWAGYSSGFHKV**	**ALMERGTEGYATDKLV**
	32	ASWAVYSSGFHKV	ALMERGTEGYELSDKLV
	33 (mo5)	**ASWAGYSSGFHKV**	**ALMERGRRDTSLTDKLV**
	34	ASWAGPLYSSGFHKV	ALMERVGGIRAWSDKLV
	35	ASWAGGSSGFHKV	AIMEGGAYRRDTSSDKLV
	36	ASWAGDSSGFHKV	ALMERVGGIRVPCPDKLV
	37	ASWALYSSGFHKV	ALMERYIGGIRAWGTDKLV
	38	ASWAGYSSGFHKV	ALMERGLYRRDTSLGDKMV
Vγ7Vδ6D2	39	ASWADSSGFHKV	ALSEQGHIYTTDKFV
	40 (mo2)	ASWADSSGFHKV	ALSELSEGYEPATDKLV
	41	ASWAGYSSGFHKV	ALSELILTGGIRATDKLV
	42 (mo1)	**ASWAYSSGFHKV**	**ALSEPWHIGGIRATDKLV**
	43	ASWAGYSSGFHKV	ALSELIGAYRRDTSSDKLV

Supplementary Table 1. Murine γδTCR chain pairs identified through the single-cell analysis

Paired CDR3γ/δ amino acid sequences (red, non-germline-encoded) identified by single-cell TCR sequencing of Btnll+6-responding murine primary Vγ7^{+} IEL. Paired sequences for which both CDR3γ and δ were found in the deep sequencing analysis are depicted in bold.

Single cell PCR		
External primer sets		
mVγ7	For	ATGCTGTGGGCTCTGG
mCγ1	Rev	TTAGGATTTCTTCTCATTGCCACAG
mVδ2-2	For	ATGGTGCGGCCGTTC
mVδ6D	For	ATGGCTCCTCAGAGCCTG
mVδ7	For	ATGGAGAGGCTGCTGTGCTCTC
mCδ	Rev	TTACAAGAAAAATAACTTGGCAGTCAAGAG
hVγ2/3/4	For	ATG**G**AGTGGGCCCTAGCG
hCγ1/2	Rev	TTATGATTTCTCTCCATTGCAGCAG
hVδ1	For	ATGCTGTTCTCCAGCCTGCTG
hVδ3	For	ATGATTCTTACTGTGGGCTTTAGCTTTTTG
hCδ	Rev	TTACAAGAAAAATAACTTGGCAGTCAAGAG
Internal primer sets		
mVγ7	For	TGAAGGCCCGGACAAGAG
mCγ1	Rev	TGTGCTCTTTCCCCATTGC
mVδ2-2	For	TGCAACGTTAAACCGCTTCTC
mVδ6D	For	AAATCCATCAGCCTTGTCATTTC
mVδ7	For	AAGCACACTGGAAGACTGACATCC
mCδ	Rev	GTCGAATTCCACAATCTTCTTGG
hVγ2-8	For	CACTGGTACCTACACCAGGAGG
hCγ1/2	Rev	GGAGGAGGTACATGTAATATGCAGAG
hVδ1	For	GGTACAAGCAACTTCCCAGCAAAG
hVδ3	For	ACCGGATAAGGCAAGATTATTCC
hCδ	Rev	GGCAGCTCTTTGAAGGTTGC
Other cloning primer sets		
mVγ5	For	ATGTCAACCTCTTGGCTTTTTC
mVδ1	For	ATGCTTTGGAGATGTCCAGTC
hVγ9	For	ATGGTGTCACTGCTCCACACATC
hVδ2	For	ATGCAGAGGATCTCCTCCCTCAT
EPCR	For	GGAGCCTCAACTTCAGGATG
EPCR	Rev	TTAACATCGCCGTCCACC
T22	For	ATGTCCTGGGTCCTCAGGG
T22	Rev	TCAAGGTGACAGTAAAGACTCGCC
Sequencing primers		
mCγ1	Rev	CCAGGATAGTATTGCCATCC
mCδ	Rev	CAGACAAGCAACATTTGTTCC
hCγ	Rev	GCAGTAGTGTATCATTTGCATC
hCδ	Rev	GGTTTTACGTGATCTGTAGAATCTGTC

Supplementary Table 2. List of primers used in this study.
All sequences read 5' to 3'. For cloning of the human Vγ chains downstream of the IRES an NcoI restriction site (C^CATGG) was introduced by mutating the first nucleotide downstream of the start codon (bold red).